Schweizerische Eidgenossenschaft
Confédération suisse
Confederazione Svizzera
Confederaziun svizra

Department of the Environment, Transport, Energy and Communication DETEC

**Swiss Federal Office of Energy SFOE**
Energy Research

**Final report 2019**

# AA-CAES-G2G

## Advanced Adiabatic Compressed Air Energy Storage grid-to-grid performance modeling

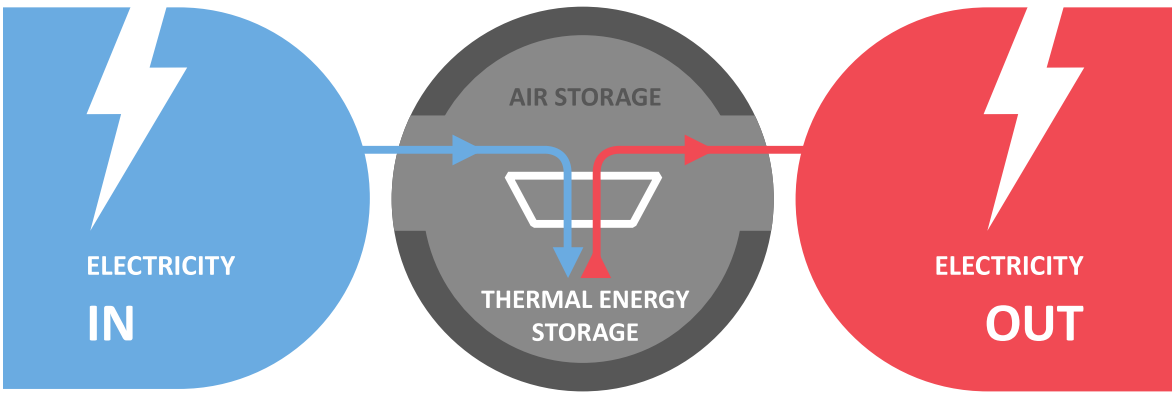





**Date:** May 31th 2019

**Town:** Bern

**Publisher:**
Swiss Federal Office of Energy SFOE
Research Programme «Electricity Technology»
CH-3003 Bern
www.bfe.admin.ch

**Agents:**
ALACAES SA
via Cantonale 19, CH-6900 Lugano
alacaes.com

ETHZ – Professorship of Renewable Energy Carriers
ML J 42.1, Sonneggstrasse 3, CH-8092 Zurich
www.ethz.ch , www.iet.ethz.ch

MAN Energy Solutions Schweiz AG
Hardstrasse 319, CH-8005 Zurich
www.man-es.com

SUPSI – DTI – MEMTi
Via Cantonale, Galleria 2, CH-6928 Manno
www.supsi.ch, www.supsi.ch/memti

**Authors:**
Maurizio C. Barbato, SUPSI – DTI – MEMTi, maurizio.barbato@supsi.ch
Davide Montorfano, SUPSI – DTI – MEMTi, davide.montorfano@supsi.ch
Filippo Contestabile, SUPSI – DTI – MEMTi, filippo.contestabile@supsi.ch
Jonathan Roncolato, SUPSI – DTI – MEMTi, jonathan.roncolato@supsi.ch
Andreas Haselbacher, ETHZ–PREC, haselbac@ethz.ch
Giw Zanganeh, ALACAES SA, giw.zanganeh@alacaes.com
Philipp Jenny, MAN Energy Solutions Schweiz AG, philipp.jenny@man-es.com
Emmanuel Jacquemoud, MAN Energy Solutions Schweiz AG, emmanuel.jacquemoud@man-es.com
Martin Scholtysik, MAN Energy Solutions Schweiz AG, martin.scholtysik@man-es.com

**SFOE head of domain:** Michael Moser, michael.moser@bfe.admin.ch
**SFOE programme manager:** Roland Brüniger, roland.brueniger@brueniger.swiss
**SFOE contract number:** SI/501589-01

**The author of this report bears the entire responsibility for the content and for the conclusions drawn therefrom.**


**Swiss Federal Office of Energy SFOE**
Mühlestrasse 4, CH-3063 Ittigen; postal address: CH-3003 Bern
Phone +41 58 462 56 11 · Fax +41 58 463 25 00 · contact@bfe.admin.ch · www.bfe.admin.ch

# Summary

The project aims to further develop a model to simulate the dynamic behavior and wire-to-wire (grid-to-grid) performance of an Advanced Adiabatic Compressed Air Energy Storage (AA-CAES) plant, by including detailed turbomachinery sub-models. Moreover, the feasibility of equipping an AA-CAES plant with a combined compressor-expander single machine was analyzed.
The project included investment and O&M costs analysis for the plant to allow their specific CAPEX and OPEX to be determined.
The novel model is now able to evaluate an AA-CAES plant grid-to-grid performance including real turbomachinery performance. Furthermore, transient processes, such as start-up and shut-down conditions, besides energy consumption during idle periods are now accounted for. The relevance of these phenomena on plant performance was found dependent on the duration of the charge-discharge cycles, being more relevant for shorter cycles.
Concerning the combined compressor-expander single machine, the analysis showed the technical unsuitability of this machine for large plants. The evaluation of plant CAPEX and OPEX was performed for a specific AA-CAES plant layout located in Switzerland and integrated in the Swiss electricity system. The plant CAPEX analysis showed that cavern excavation is 52% and turbomachinery 32% of total investment. Thermal energy storage is just 6% of plant costs.

# Riassunto

Il progetto mira allo sviluppo di un modello di simulazione del comportamento dinamico e delle prestazioni wire-to-wire (grid-to-grid) di un impianto Advanced Adiabatic Compressed Air Storage (AA-CAES), includendo dei sottomodelli dettagliati per le turbomacchine. Inoltre, il progetto include l'analisi della fattibilità di dotare un impianto AA-CAES di una macchina singola combinata per la compressione-espansione.
Il progetto infine comprende l'analisi dei costi di investimento e di O&M per l'impianto così da consentire la determinazione di CAPEX e OPEX.
Il nuovo modello è ora in grado di valutare le prestazioni di un impianto AA-CAES da grid-to-grid, comprese le prestazioni reali delle turbomacchine. I processi transitori, come le condizioni di avvio e di arresto, oltre al consumo di energia durante i periodi di semplice stoccaggio sono ora considerati. La rilevanza di questi fenomeni sulle prestazioni dell'impianto è risultata dipendente dalla durata dei cicli di carica-scarica, essendo essi più influenti per cicli più brevi.
Per quanto riguarda la macchina combinata compressore-espansore, l'analisi ha evidenziato l'inadeguatezza tecnica di questa macchina per impianti di grandi dimensioni. L'analisi CAPEX/OPEX è stata effettuata per uno specifico layout di impianto AA-CAES situato in Svizzera e integrato nel sistema elettrico svizzero. L'analisi CAPEX ha mostrato che lo scavo della caverna e le turbomacchine rappresentano rispettivamente il 52% e il 32% del totale dei costi. Il sistema di stoccaggio dell'energia termica incide, invece, solo per il 6% sui costi totali.

# Zusammenfassung

Das Projekt hat das Ziel, ein Modell weiter zu entwickeln, mit welchem das dynamische Verhalten einer am elektrischen Netz angeschlossenen adiabatischen Druckluftspeicheranlage simuliert werden kann. Das Modell beinhaltet detaillierte Untermodelle für das Verhalten der Turbomaschinen. Im Weiteren wurde die Machbarkeit einer adiabatischen Druckluftspeicheranlage, die mit einer kombinierten Verdichter-Expander Einheit ausgestattet ist, untersucht. Schlussendlich wurde ein detailliertes Kostenmodell erstellt, um die spezifischen Investitions- und Unterhaltskosten der Anlage zu bestimmen.
Das neue Modell ist in der Lage, das Verhalten einer am elektrischen Netz angeschlossenen adiabatischen Druckluftspeicheranlage mit realistisch abgebildeten Turbomaschinen zu berechnen. Transiente Prozesse wie das Herauf- und das Herunterfahren der Anlage werden nun durch deren Dauer und Energieverbräuche, auch während der Ruhephasen, berücksichtigt. Es stellte sich heraus, dass diese Prozesse für das Verhalten der Anlage dann relevant sind, wenn die Dauern der Lade-/Entladezyklen kurz sind.
Die Analyse von kombinierten Verdichter-Expander Einheiten zeigte, dass diese für grosse Anlagen nicht geeignet sind.

Die Investitions- und Unterhaltskosten wurden für eine spezifische, ins schweizerische Elektrizitätsnetz integrierte, Anlagenkonfiguration bestimmt. Die Anteile des Kavernenaushubs und der Turbomaschinen an den Investitionskosten betragen 52% respektive 32%. Der thermische Energiespeicher trägt nur 6% zu den Investitionskosten bei.

# Content

# 1 AA-CAES physical model

## 1.1 Introduction

Advanced Adiabatic Compressed Air Energy Storage (AA-CAES) systems store electric energy by pressurizing air: high-pressure air is stored in underground caverns and its thermal energy, increased by the compression, is stored in thermal-energy storages (TES). Electric energy can be recovered by expanding high-pressure hot air in a turbine. The AA-CAES technology should be feasible to operate in the energy storage market and grid ancillary services.
With the objective of defining grid-to-grid performance of a realistic AA-CAES plant, this work aims at investigating how real efficiencies maps of compressor and turbine would affect the plant performance. Furthermore, the effects of turbomachinery transients were also studied.

## 1.2 Physical model description

To simulate an AA-CAES plant, the approach used is to apply a tool capable of solving differential equations derived from the mathematical model of a system that evolves in time. The model was built and solved in the Matlab-Simscape environment. To describe the topology of this model, we started from the schematic of an AA-CAES plant as reported in Figure 1. In this figure, two turbomachinery trains are indicated: the compressor train on the left-hand side, where a motor moves the low-pressure and a high-pressure compressors (LPC and HPC, respectively); the turbine train on the right-hand side, where the high-pressure and low-pressure turbines (HPT and LPT, respectively) are connected to a generator. The plant includes a volume called Chamber or TES Chamber that hosts the low-pressure TES (LP-TES) and a cavern that contains the high-pressure TES (HP-TES) and stores the cold pressurized air. In the schematic, an intercooler is located before the HPC. Figure 2 shows the correspondent numerical model realized with customized blocks in Matlab-Simscape.

During charging, the AA-CAES plant exploits electric energy to compress ambient air, i.e., converts electric energy into thermal and mechanical energy. Air sucked from the environment passes through the LPC then transfers its thermal energy to the LP-TES. Afterwards, the air flows to the HPC passing through an intercooler where it is cooled only if its temperature exceeds a fixed pre-specified value. In the HPC, air is further compressed and sent to the cavern where it leaves its thermal energy in the HP-TES and it is stored at a low temperature.

When the AA-CAES is required to produce electric energy, the high-pressure cold air is heated in the HP-TES and then sent to the HPT for a first expansion. After that, the air is reheated in the LP-TES and flows to the LPT for the final expansion. The turbine train drives a generator that delivers electric energy.

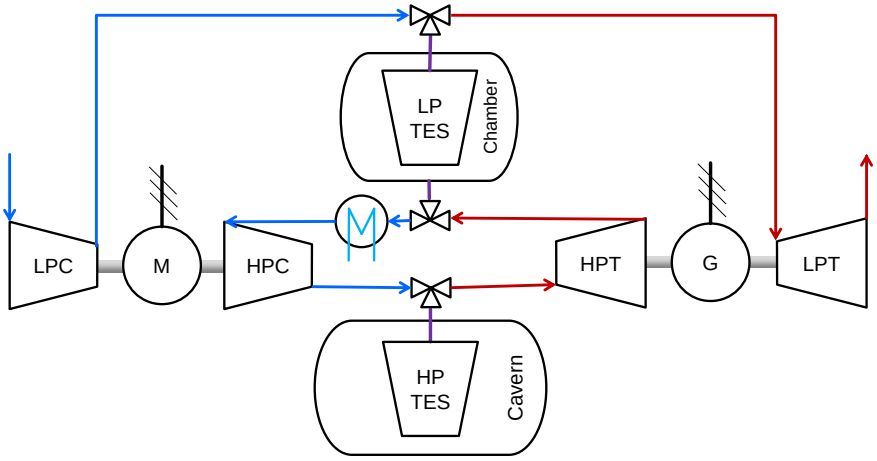


**Figure 1: AA-CAES plant schematic.**

Figure 2 shows the simulation model built for the AA-CAES plant shown in Figure 1 and realized with customized blocks in Matlab-Simscape. The equations behind the Matlab blocks are reported in the following. The power absorbed by the compression train is described by equations (1), (2) and (3) considering that the total power available is distributed between LP and HP compressors. The adiabatic compression of air can be modelled through a polytropic efficiency, as reported in Eq.(4) or, alternatively, by an isentropic efficiency, as described in Eqs. (5) and (6). For these transformations, the ratio of specific heats was assumed constant and it was determined as the average between the initial and final process values.

During the discharging of the plant, mechanical power is extracted from the hot air flow passing through the turbines connected to the generator. By analogy to the compressors, adiabatic expansions can be modelled either through a polytropic efficiency as specified by Eq. (8), or an isentropic efficiency, as shown by Eq. (9). The electric generator is modeled by taking into account its efficiency, as shown by Eq. (7). Depending on the scheduling of the plant in the physical model, turbomachinery can be controlled either by specifying the electric power input of the compressor train and turbine activation or alternatively assigning the mass flow rates during charging and discharging.

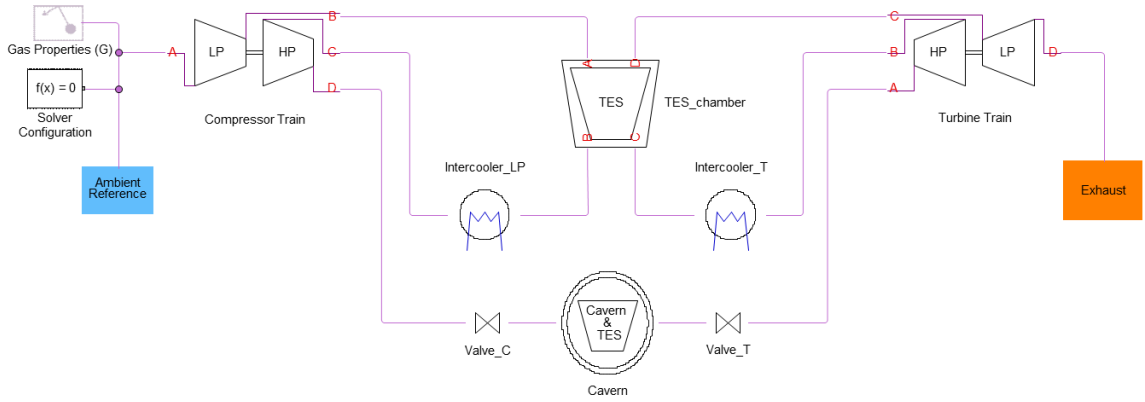


**Figure 2: AA-CAES plant shown in Figure 1 as implemented in Simscape.**

$$\dot{P}_C = \dot{P}_{C,LP} + \dot{P}_{C,HP} \tag{1}$$

$$\dot{P}_{C,LP} \cdot \eta_m = \dot{m} \cdot \Delta h = \dot{m} \cdot (h_{out} - h_{in}) \tag{2}$$

$$\dot{P}_{C,HP} \cdot \eta_m = \dot{m} \cdot \Delta h = \dot{m} \cdot (h_{out} - h_{in}) \tag{3}$$

$$T_{out} = T_{in} \left(\frac{p_{out}}{p_{in}}\right)^{\frac{\gamma-1}{\gamma \cdot \eta_{pol}}} \tag{4}$$

$$T_{out,is} = T_{in} \left(\frac{p_{out}}{p_{in}}\right)^{\frac{\gamma-1}{\gamma}} \tag{5}$$

$$\eta_{is} = \frac{h_{out,is} - h_{in}}{h_{out} - h_{in}} \tag{6}$$

$$\frac{\dot{P}_T}{\eta_m} = \dot{m} \cdot \Delta h = \dot{m} \cdot (h_{in} - h_{out}) \tag{7}$$

$$T_{out} = T_{in} \left(\frac{p_{out}}{p_{in}}\right)^{\frac{\gamma-1}{\gamma} \cdot \eta_{pol}} \tag{8}$$

$$\eta_{is} = \frac{h_{in} - h_{out}}{h_{in} - h_{out,is}} \tag{9}$$

Heat exchangers were modelled as components that guarantee a defined maximum or minimum temperature. This characterization aimed at the determination of the power that should be removed from or added to the air flow to keep the temperatures in the selected ranges. The TES chamber and cavern were assumed to have constant volumes. The first one is the chamber that accommodates the LP TES while the second one is the cavern that contains the HP TES and stores the pressurized air.

The dynamics of both these volumes was modeled implementing the conservation of mass and energy, as shown in Eqs. (10) and (11) respectively. The former states that the mass variations within

the volumes are determined by the balance of incoming and outgoing mass flow rates connected to the plant operations and the mass flow rate due to leakages that might occur.

The energy balance for the cavern is given in Eq. (11). The variation of the internal energy in the cavern depends on the enthalpy flows linked to the mass flow rates cited above and to the heat transfer occurring between the stored air and the cavern walls. Convective thermal losses at the cavern walls surface were accounted for assuming an average area and a constant heat-transfer coefficient.

The last term on the right side of Eq. (11) takes into account the thermal loss between TES walls and cold stored air. For non-adiabatic TES systems, this term is specifically calculated by the TES sub-model.

$$\frac{dM}{dt} = \dot{m}_{in} - \dot{m}_{out} - \dot{m}_{leakages} \tag{10}$$

$$\frac{dU}{dt} = [\dot{m} \cdot h]_{in} - [\dot{m} \cdot h]_{out} - [\dot{m} \cdot h]_{leakages} - h_c A(T - T_{wall}) + \dot{Q}_{TES,loss} \tag{11}$$

Air was assumed to be dry and behaving as an ideal gas with temperature-dependent properties [1].

## 1.3 Turbomachinery modelling

Part of the modeling efforts were focused on the improvement of turbomachinery modelling, which included the energy required for the transients (start-ups and shut-downs) and the integration of the efficiency maps of compressors and turbines. The modeling approaches adopted are described in the following sections.

### 1.3.1 Transients and idle periods

In the analysis of suitable turbomachinery, constant speed machines were considered for both compressors and turbines. This choice was preferred to the more expensive solution of variable speed components which would require dedicated electronics equipment such as Variable Frequency Drives. The performance flexibility of turbomachinery, whenever possible, is guaranteed by systems that include variable valve opening and variable inlet guide vanes. Details on turbomachinery are reported in Chapter 4.

When dealing with turbomachinery transients, such as start-ups, it is useful to distinguish between two phase:

- a mechanical start-up phase, during which the turbomachinery speed accelerates from 0 rpm to a nominal speed at off-design process conditions.
- a process/thermodynamic start-up phase, during which the turbomachinery, at constant RPM, reaches the operating point starting from off-design conditions. The duration of this process depends on the specific machine.

To avoid frequent and costly machines start and stop, the possibility of letting the compressor or turbine train rotate during idle (i.e., when the plant is neither storing nor producing electric energy) was examined. Unfortunately, the energy necessary to maintain the turbomachinery train rotating synchronously with the grid during an idle (i.e., 3000 rpm for 50 Hz) is not negligible and this procedure was considered not sustainable. A possible strategy to have frequent startup cycles could be to adopt “over-dimensioned” electrical motors. This should also shorten the startup period and preserve components life. A direct-drive is foreseen for the LP turbomachinery while a gearbox might be useful for HP turbomachinery to let them run at higher speeds. The inclusion of gearboxes will increase turbomachinery train inertia and costs. A detailed technical discussion about start-ups and shut-down of turbomachinery is reported in Section 14.4.

**Realistic compressor train start-up procedure**

For an AA-CAES plant with multiple compressors and multiple TES, the compression train start up procedure is not simple. Figure 3 illustrates the schematic of the compression branch in the AA-CAES, including the auxiliary components for the management of transients. After the mechanical start-up, i.e., the initial acceleration of the LPC, to reach the required compression ratio (given by the TES chamber pressure), the variable guide vanes are used to modulate the mass flow rate passing through the compressor. The mass flow rate exiting the LPC is sent to a blow-off valve (BOV), letting the compression ratio of the compressor increase. The goal is to reach the wanted value at the lowest mass flow rate. This phase is performed with valves V1 and V2 closed, therefore, no mass passes though TES1 (LP-TES) and HPC.

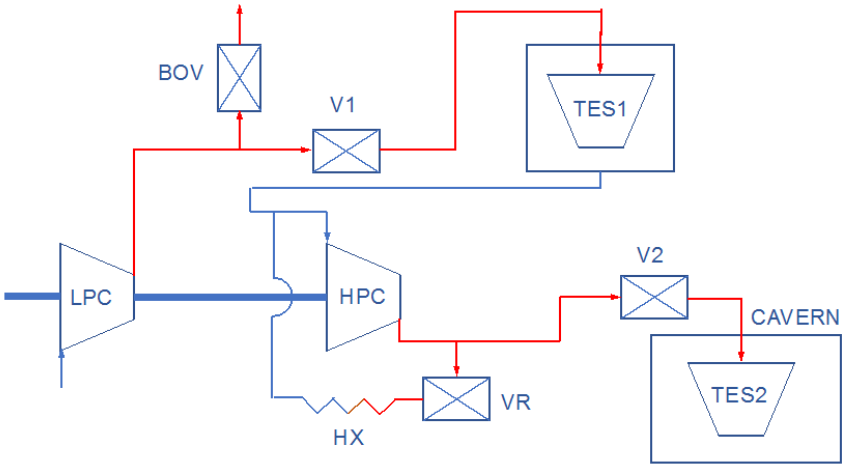


**Figure 3: Schematic of the physical layout of the compression branch in the AA-CAES plant layout**

Once the wanted compression ratio is achieved in the LPC, the blow-off valve BOV is closed gradually while valve V1 is opened, letting the air flow through the TES 1 and then though the HPC. Here, exploiting the variable guide vanes and a compressed air recirculation through valve VR, provided compressed air cooling in the heat exchanger HX, the HPC is brought to its expected compression ratio. The pressurization of the VR ducts exploits the mass flow coming from the LPC, in order to do not let the TES1 chamber pressure drop. Then V2 is opened and the mass flow rate passing through the compressor train is increased up to the wanted value (corresponding to the available power from the grid). Air, passing through valve V2, goes into TES 2 and then, once cooled, into the cavern. The

decision to turn on the LPC before and the HPC after or, alternatively, simultaneously should be part of the process optimization of the plant.

**Realistic turbine operation**

Moving to the turbine side, some operating scenarios were identified:

a) The HPT is throttled, i.e. its inlet pressure is kept constant by a throttling valve. As a consequence, the HPT and LPT can work at constant inlet pressure. There are no problems with the grid power injection (a constant production power can be guaranteed), but some extra losses and round-trip efficiency reduction have to be expected. This is the operative modality exploited at Huntorf [12].
b) The HPT and LPT operate with inlet pressures that depend on the cavern pressure. In this case, the HPT inlet pressure is not constant and, even if the air mass flow rate is kept constant, the electric power produced is neither constant.

**Modelling approach for transients**

After an accurate analysis of transient procedures (see Chapter 4 for details), the idea of having a detailed modeling of turbomachinery transients was considered to be not very convenient. Detailed modeling and the consequent computational effort were considered to be not worth it especially when compared with less detailed approaches that can already provide the information needed for evaluating the AA-CAES plant performance. The alternative and simpler approach considers the energy spent and the time required for typical turbomachine start-ups, without the need of physical modelling of all the components shown in Figure 3.

The data needed for this simplified model originates from real machines performance data that were brought by MAN Energy Solutions Schweiz AG (MAN ES). The “slow roll” (see Section 4.4) was considered the most suitable option for an AA-CAES plant. This option avoids too-long transients strictly connected to the thermal inertia of the components, which would also affect the responsiveness of the AA-CAES plant. In fact, turbine start-up after a shut-down requires much longer time due to thermal inertia of the turbomachine itself and of the lubricating oil system. The “slow roll” option implies keeping the machine warm and slowly rotating it with a relatively small power consumption.

### 1.3.2 Compressors performance maps

The AA-CAES plant performance is obviously affected by performance of the turbomachines. Therefore, the compressor and turbine performance need to be included in a model that wants to closely reproduce plants behavior and therefore be useful for evaluating the integration of a plant in the electric grid.
For the compressors, their efficiency maps were included in the AA-CAES plant model by providing the polytropic efficiency as function of the volumetric flow rate and the compression ratio. Volumetric flow rate was preferred to the mass flow rate in order to take into account also appreciable density variations related to pressure variations within the TES chamber.
Performance maps of turbomachinery are typically given as lines in the volume flow rate vs compression ratio plane where efficiency regions are also drawn. To use these data in a model where machines working conditions can span over a wide envelope, the performance maps were rebuilt to ensure that also zones outside the normal operation region could be numerically accessed during the simulations. In other words, for compressors, regions beyond the surge and choke lines, must be represented and smoothly connected with normal operation regions. The compressor polytropic efficiencies were therefore interpolated by a polynomial surface to increase the numerical stability. Figure 4 and Figure 5 depict the contour plot of the LPC and HPC efficiency maps, respectively. The normal operating regions are those enclosed by the dashed white lines.

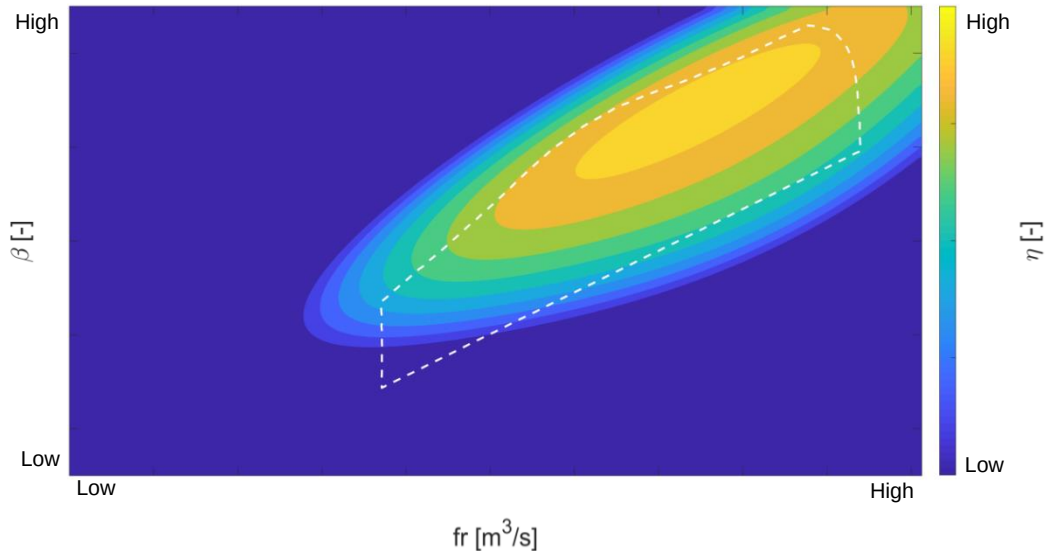


**Figure 4: LPC efficiency map (normal operating region enclosed by the dashed white line).**

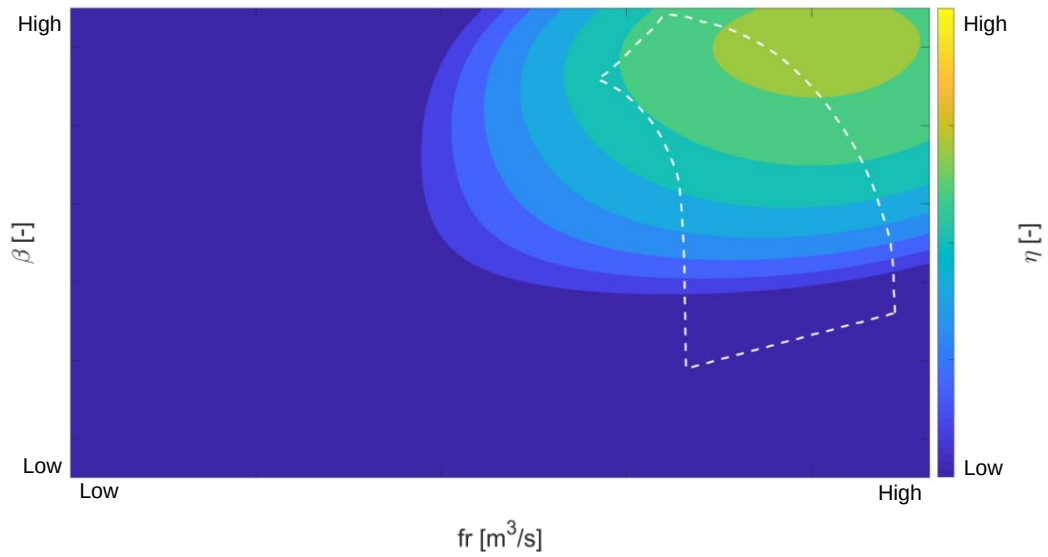


**Figure 5: HPC efficiency map (normal operating region enclosed by the dashed white line).**

### 1.3.3 Turbines modelling and performance maps

The turbines efficiency maps where extended with the same strategy pursued for compressors. In this case, the polytropic efficiency was represented in a plane with the compression ratio on the ordinate axis and the reduced mass flow rate $G_R$ on the abscissas. The reduced mass flow rate is defined by Eq. (12).

$$G_R = \frac{\dot{m}\sqrt{T_{in}}}{p_{in}} \tag{12}$$

In an AA-CAES plant, turbines are requested to work with variable temperature and pressures at their inlets. These properties affect very much the mass flow rate and this is also the rationale for choosing the reduced mass flow rate to describe the turbine performance. In this project, the idea of exploring different levels of maximum pressure in the cavern was pursued.

The normal operating ranges for both the turbines were extracted from the data provided by MAN Energy Solutions Schweiz AG, computing the reduced mass flow rates; they are depicted with black dashed lines in the expanders efficiency maps (see Figure 7).
The idea of implementing throttling valves before the expanders, so as to guarantee a constant pressure at the HPT inlet, was evaluated. These components were finally not considered to prevent efficiency losses (of up to 4%). As a direct consequence of this approach, neither the turbine power nor the mass flow rate during the discharging phases of the plant were constant: in other words, as it will be seen in the following, the AA-CAES plant output power depends on plant dynamics and turbines characteristics.

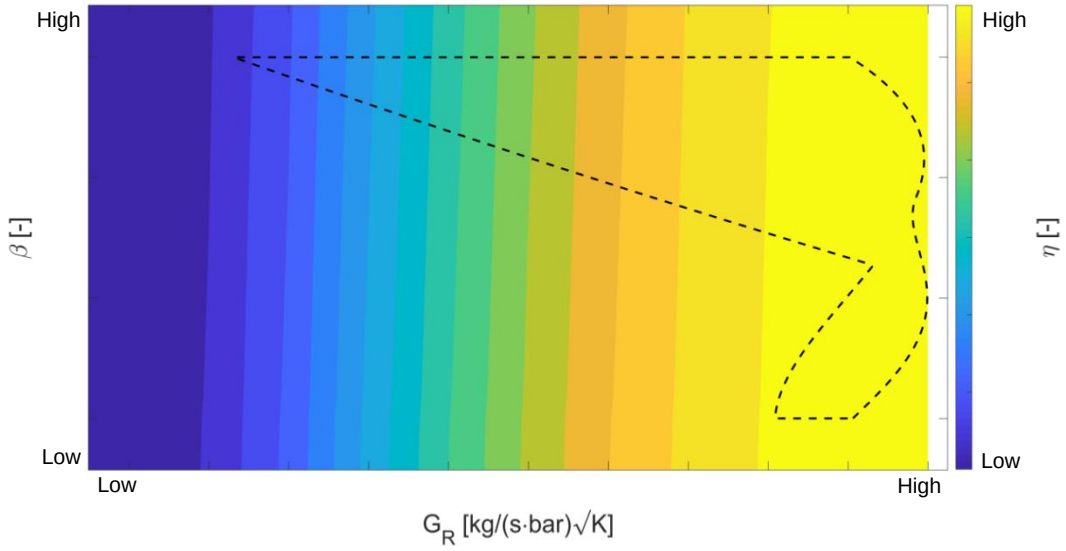


**Figure 6: LPT efficiency map, zoom (normal operating region enclosed by the dashed black line).**

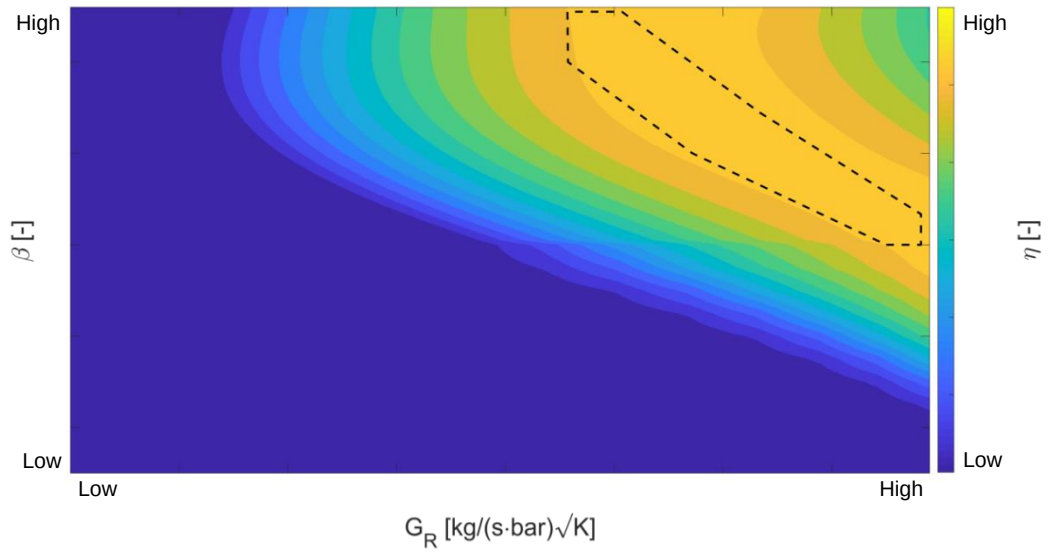


**Figure 7: HPT efficiency map (normal operating region enclosed by the dashed black line).**

# 2 AA-CAES economic analysis

The AA-CAES cost model was set up taking into consideration the plant's main components, such as civil works, turbomachinery, and thermal energy storage units, as well as other necessary components for the balance of the plant (transformer, hardware/software, cabling), piping, valves, and auxiliary systems (plant ventilation, safety and monitoring).
The turbomachinery data were provided by the G2G project partner MAN Energy Solutions Schweiz AG, the thermal energy storage costs are provided by ALACAES from their past experience in constructing such units. The civil works costs were provided by Geostock, the world leader in design and construction management of hydrocarbon mined rock storage facilities, in the framework of an on-going collaboration between ALACAES and Geostock. The civil works costs were consolidated into a lump-sum in order to respect the NDA in place with Geostock.
The base case of the cost model was set up for a plant with 100 MW power (100 MW discharging, 135 MW charging) and 500 MWh capacity in Swiss Alpine rocks. The capital expenditure per kWh of installed capacity for this base case is 200-300 €/kWh. As seen further below, this figure changes depending on location, available rock quality, as well as pressure and power range.

The O&M costs for the turbomachinery are difficult to estimate since the daily start-up and shut-down cycles are not common in the industry. Further, they depend on location specific factors such as process air quality and temperature. Nevertheless, a yearly O&M cost of 2-3%of the turbomachinery CAPEX is considered reasonable. For the civil works and the sealing system, the O&M costs are 3% of the civil works' CAPEX, while the TES will have smaller O&M costs due to the lack of moving parts. For the total plant, a yearly O&M cost of 2.5% is found to be reasonable.
Figure 8 shows the macro cost structure for a reference plant with 100 MW power output and 500 MWh capacity. The civil works and the turbomachinery have by far the biggest share of the plant costs.

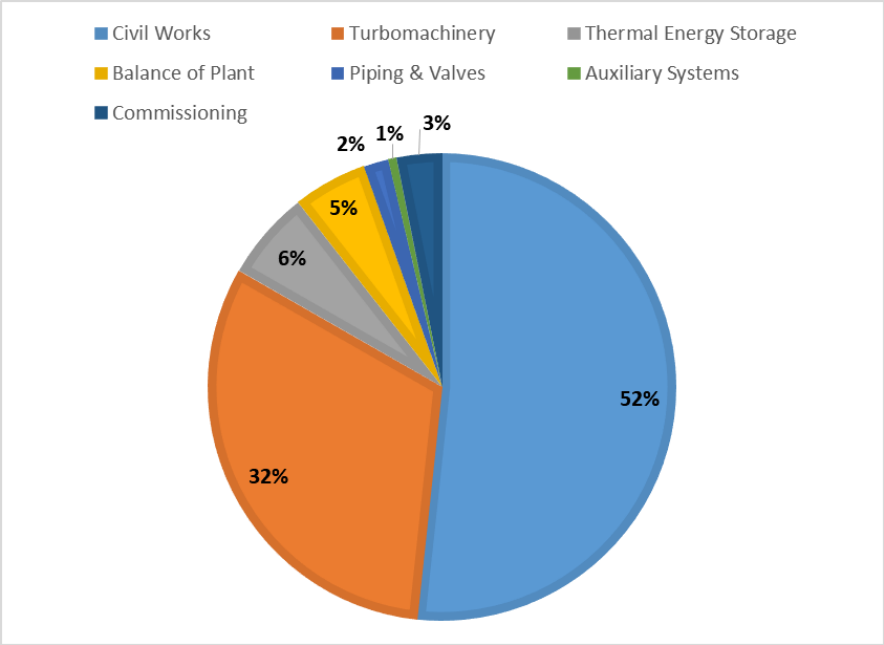


**Figure 8: Macro cost structure for a reference AA-CAES plant.**

Table 1 shows the CAPEX per kWh of installed capacity for the reference plant for different locations and rock qualities. The main driver for lower costs in developing countries is the lower cost of civil and construction works, while higher quality rocks reduce the costs by allowing larger cavern cross sections and less rock support.

**Table 1: CAPEX per kWh of installed capacity for the reference AA-CAES plant for different economies and rock qualities**

| CAPEX [€/kWh] | High Quality Rock | Low Quality Rock |
|---|---|---|
| **Developed Countries** | 200-300 | 200-300 |
| **Developing Countries** | 100-200 | 100-200 |

Finally, CAPEX estimations are done for plant configurations with different plant power ratings and pressure ranges, but the same plant capacity of 500 MWh. The results are summarized in Table 2. Reducing the plant power rating results in lower turbomachinery costs (but would increase the charging/discharging time, which is not reflected in the CAPEX). Reducing the pressure range increases the necessary cavern volume - and hence the civil works cost - to obtain the same plant capacity.

**Table 2: CAPEX per kWh of installed capacity for a 500 MWh AA-CAES plant with different power ratings and pressure ranges (developed country, high rock quality)**

| CAPEX [€/kWh] | $p_{max}$ = 100 bar | $p_{max}$ = 60 bar |
|---|---|---|
| **$P_{out}$ = 100 MW** | 200-300 | 200-300 |
| **$P_{out}$ = 50 MW** | 100-200 | 200-300 |

Table 3 shows a comparison of different energy storage technologies from the point of view of efficiency, cycle lifetime (how many cycles the storage technology can do during its lifetime) and capital costs. While AA-CAES has a lower efficiency compared to pumped hydro storage (PHS), it also has lower costs. Further, it has a significantly smaller environmental footprint since all the installations are underground and no dams and artificial lakes need to be created. Further, PHS competes with drinking and agricultural water supply in regions where these are scarce. Beyond these points, PHS and AA-CAES have many similarities: similar response times, similar dimensions required for profitable operation, modular units not feasible, etc.

While Li-ion batteries have higher efficiencies, they are also considerably more expensive and have much lower cycle lifetime, which means that the capital investments need to be amortized in a much shorter time frame. However, it is also important to note that due to Li-ion batteries' very fast response times, they can be used for use cases where AA-CAES and PHS are not adequate, such as frequency regulation.

Redox flow batteries do not have any significant advantages compared to other storage technologies, but can be scaled more easily with respect to Li-ion.

**Table 3: Comparison of cycle efficiency, cycle lifetime and capital costs of different energy storage technologies**

| | Efficiency | Cycle Life at Depth of Discharge (DoD) | | | Capital Cost [€/kWh] |
|---|---|---|---|---|---|
| | | 100% | 80% | 33% | |
| **AA-CAES** | 75% | > 25'000 DoD independent | | | 200-300 |
| **Pumped Hydro Storage** | 85% | > 25'000 DoD independent | | | 240** |
| **Li-ion Battery** | 90% | 4000* | 6000* | 8500* | 590** |
| **Vanadium Redox Flow Battery** | 75% | 2900* | 3500* | 7500* | 660** |

* Ref. [3].

** Lazard's Levelized Cost of Storage, 2016

Another important comparison of energy storage technologies can be found looking at their environmental impact. A study by Barnhart and Benson (see Ref [3]) looked at a metric called Energy Stored on Invested (ESOI), that represents the ratio of electrical energy stored over the lifetime of a storage device to the amount of primary embodied energy required to build the device. Figure 9 shows the ESOI for various energy storage technologies. CAES has the best performance and Lead Acid batteries the worst. Generally it can be seen that battery storage technologies have significantly lower ESOI values, meaning that they are much more energy intensive to produce. The best performing battery, Li-ion, can store throughout its lifetime 10 times the energy that has been used to build it, while the value for CAES is 240. The authors suggest that in the best case, with improvements in mining of the raw materials used for batteries and technological advancements in battery technologies in general, the values could increase by maximum a factor of 3. This means that the ESOI for Li-ion batteries can potentially reach 30 in the future, hence still being an order of magnitude worse than CAES and PHS

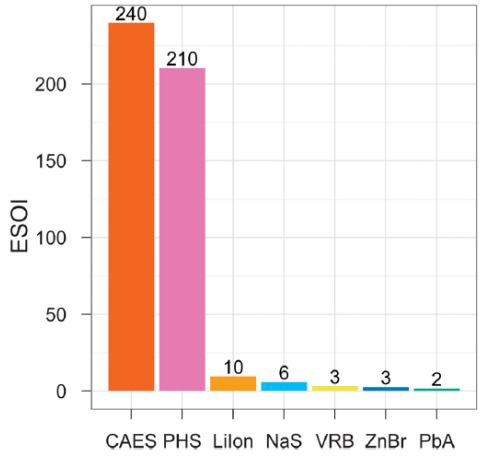


**Figure 9: ESOI the ratio of total electrical energy stored over the life of a storage technology to its embodied primary energy. Higher values are less energy intensive.**

Despite the economic and environmental advantages of AA-CAES demonstrated in this chapter, there are still no commercially operating plants available. There are several reasons for this:

- High capital investment requirements: AA-CAES plants are economically attractive only above a certain size (~20 MW/50 MWh). At the same time the technology is not fully proven yet, hindering traditional investment vehicles to invest in the technology. This creates a deadlock situation for the commercialization of the technology. Therefore, in order for the technology to become commercial, either government funds or visionary wealthy private investors are necessary to finance a first semi-commercial demonstration plant. However, these have proven to be very hard, if not impossible, to obtain.

- Curtailment subsidies: Currently wind parks and PV farms in most of the regions of the world are subsidized for curtailment, meaning that they are paid the electricity price even if the grid operator orders them to shut down the plant due to over-production. These curtailment costs (370 Mio. € in Germany in 2016 alone, 420 Mio € in UK in last five years) are subsidized by the tax payers and create a strong lack of incentive for energy companies to invest in energy storage. ALACAES has met several Swiss and European wind park operators that stated this as the main reason why they are not interested in investing in storage.

- Regulatory environment: the electricity markets are not designed to accommodate energy storage plants. The very strict rules for participants to electricity and reserve markets creates a barrier for the entrance of new technologies to the field. For instance, AA-CAES plants will most probably have slight fluctuations in the power output during the charging/discharging cycles. However, grid operators do not tolerate any deviation from the committed amount of power by the provider and failure to comply entails strong financial punishments and exclusion from the market. Also battery technologies are best suited for short term frequency regulation and not continuous production, making it difficult for them to comply with the operators' rules of committing the power for a certain pre-defined amount of time.

However, recently the interest in alternative storage technologies is increasing, with the Huntorf plant (the first ever built CAES plant) announcing plans to increase their capacity due to increasing demand. On the other hand, some grid operators started making exceptions from their established rules for new technologies, for instance not requiring 15 min availability for battery storage plants serving the secondary reserve market. Similar new rules can also help the adoption of AA-CAES in the electricity grid.
We further encourage the funding institutes such as the Federal Office of Energy to adopt financing schemes that are more favorable for the private sector, such as granting higher percentages of the project costs and accommodating funding for semi-commercial projects. This will reduce the risks for industrial investors that want to participate to the development of new technologies but are hindered due to high risk and capital requirement. Otherwise the commercialization of AA-CAES will be very difficult.

# 3 AA-CAES integration in Swiss grid

With support from the SCCER HaE, we have begun investigating the siting of an AA-CAES plant in Switzerland and the integration of an AA-CAES plant in the Swiss electricity system. The AA-CAES activities in the SCCER HaE and the SFOE AA-CAES projects benefit significantly from each other.

## 3.1 AA-CAES plant siting

Regarding the investigation of the siting of an AA-CAES plant in Switzerland, our original objective was to reuse unused military caverns. The rationale was that depending on the volume of unused military caverns relative to the required cavern volume for a given plant capacity, reusing unused military caverns would at least reduce and perhaps even eliminate the cost of excavating a cavern. In Figure 10, the cavern sites obtained from Armasuisse are shown along with 220 and 380 kV grid nodes and circles indicating 5 and 10 km radii from the grid nodes. Closer investigation of the list of unused military caverns showed that none of them were large enough for our target cavern volume of 177'000 $m^3$. In fact, most of them were so small that the cost savings were not significant compared to the total plant capital costs. The associated estimated costs of enlarging the current caverns to the target volume and connecting them to the nearest grid node is presented in Figure 11, assuming an excavation cost of 150 CHF/ $m^3$ and a connection cost of 125 kCHF/km.[1]

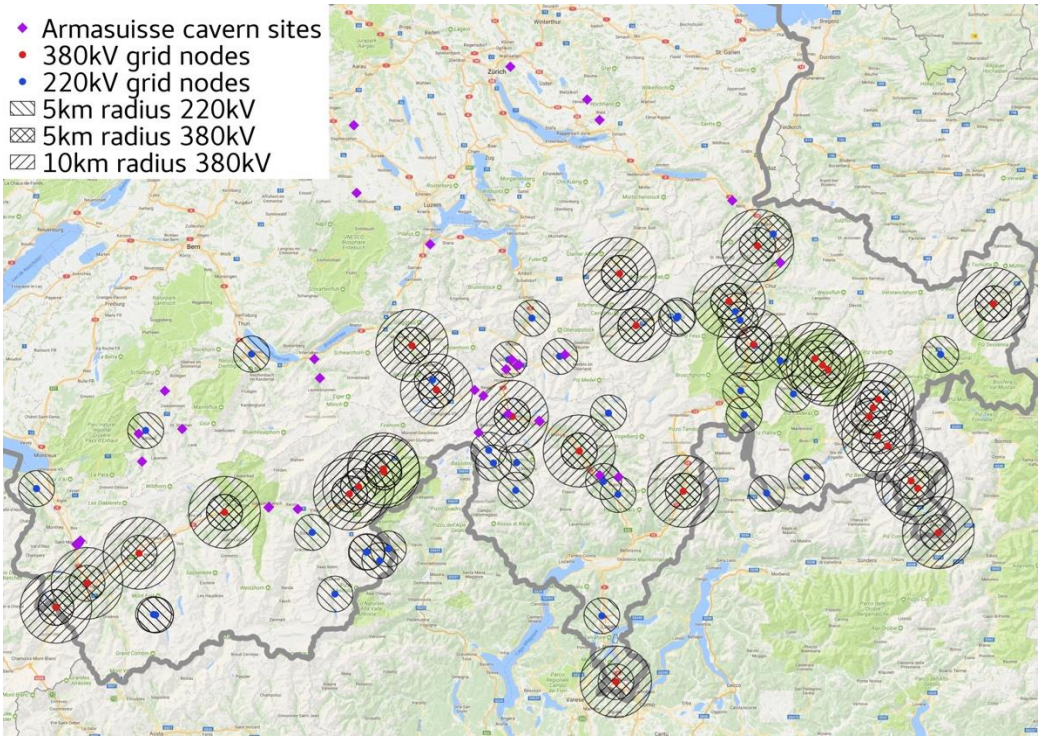


**Figure 10: Cavern sites obtained from Armasuisse, superimposed on map with 220 and 380 kV grid nodes and circles with 5 and 10 km radii to indicate distance from the grid nodes.**

[1] In estimating these costs, we assumed an average cavern height of 3 m. This estimate was necessary because the information obtained from Armasuisse contained only the floor area of the caverns, but not their volumes.

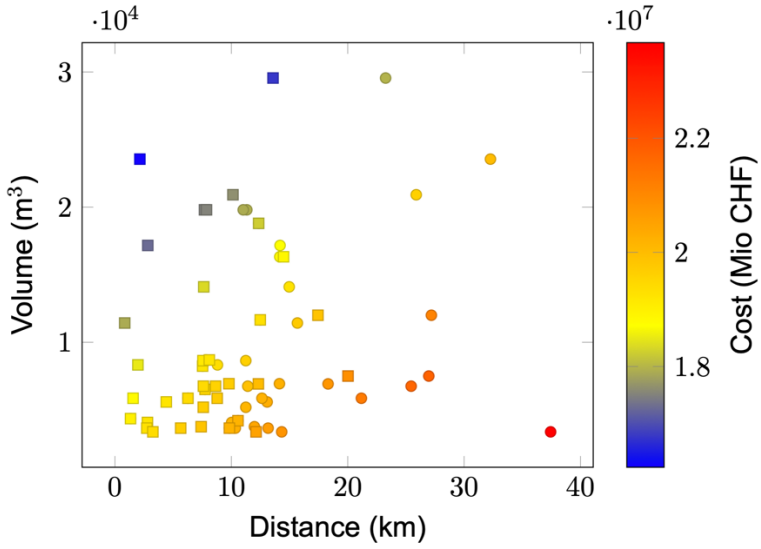


**Figure 11: Cost in MCHF of enlarging caverns shown in Figure 10 from their current volumes to the target volume of 177'000 m$^3$ and connecting them to the nearest grid node, from [2].**

Furthermore, discussions with Armasuisse and Amberg Engineering revealed further disadvantages of reusing unused military caverns:

1. The caverns do not have sufficient overburden to contain the maximum cavern pressures of about 100 bar.
2. The caverns typically have multiple entrances and exits, all of which represent potential paths for air to leak from the cavern.
3. The caverns are typically highly branched, leading to large surface-to-volume ratios, which would increase heat losses from the compressed air to the surrounding rock.
4. The cross-section of most of the caverns is horseshoe-shaped, which may induce stress concentrations and consequent fracturing and air leaks.
5. Few caverns were located in regions with high-quality rock (the Aare massif), and they would therefore likely have required costly measures to render them airtight.

For these reasons, the plant-siting study has shifted attention to excavating entirely new caverns. The financial consequences of this decision on the profitability of AA-CAES plants in Switzerland will be investigated in the ongoing SCCER HaE AA-CAES project. The consequences are unlikely to be significant because Figure 11 shows that excavating an entirely new cavern and connecting to a grid node that is about 40 km away is a small fraction of the total plant cost.

## 3.2 AA-CAES plant integration in the Swiss grid

As far as the integration of an AA-CAES plant in the Swiss electricity system is concerned, we are collaborating with researchers from the Future Electricity Network group at the Energy Science Center at ETH. In this collaboration, we use a nonlinear alternating current power flow model that includes multi-period dispatch optimisation to simulate the interconnected electricity systems of Switzerland, Germany, France, Italy, and Austria and model the AA-CAES plant through its power ratings, its capacity, efficiency, and ramp rates Including in this grid model the detailed plant model being developed at SUPSI is not an option because the resulting simulations would be too time-consuming.

In the first set of simulations, see [4], we investigated the eight plant sites listed in Table 4 and shown in Figure 12. The sites were selected because existing military caverns were located close to grid nodes, see Figure 10. For each of the sites, an optimisation was carried out to achieve the lowest

economic dispatch cost of the available electricity generators within the limits of the generator fleet and transmission network. The power-grid representation in the optimisations included the full Swiss high-voltage transmission network as well as an aggregated representation of Germany, France, Italy, and Austria. While the transmission network and generation fleet within each of the neighboring countries was aggregated, all cross-border transmission lines were represented in detail. Since Switzerland is highly interconnected with its neighboring countries, it is critical to capture the neighboring countries' generators and costs. The representation of the Swiss power grid was based on data from the Swissmod model [5].

**Table 4: Plant sites and associated grid node names and numbers used in first set of simulations.**

| Cavern ID | Latitude | Longitude | Node Name | Node Number |
|---|---|---|---|---|
| 31004 | 46.654 | 8.616 | Goeschenen | 78 |
| 1007 | 46.668 | 8.596 | Goeschenen | 78 |
| 1181 | 46.301 | 7.717 | Chippis | 35 |
| 1212 | 46.297 | 7.823 | Bitsch | 48 |
| 1679 | 46.670 | 7.883 | Wimmis | 34 |
| 1220 | 46.485 | 7.249 | Gstaad | 23 |
| 1221 | 46.496 | 7.406 | Gstaad | 23 |
| 1247 | 47.080 | 8.036 | Littau | 62 |
| 32005 | 46.211 | 7.032 | St. Triphon | 14 |
| 32008 | 46.208 | 7.029 | Batiaz | 13 |

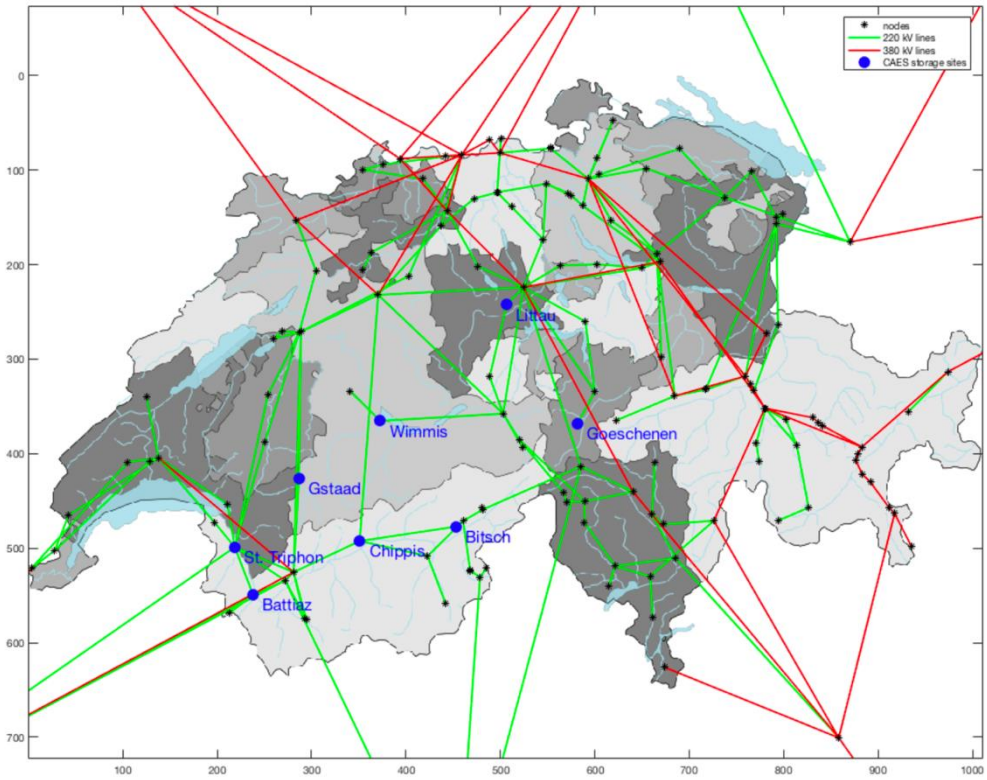


**Figure 12: Plant sites and power-grid representation in first set of simulations.**

The results from the first set of simulations showed that a 100 MW/500 MWh AA-CAES plant was heavily used in the dispatch, exploited the transmission network to a greater degree, and achieved dispatch cost savings compared to the option without the plant.

Building on these promising initial results, the second set of simulations focused on AA-CAES plants located at the grid node near Bitsch, see Garrison et al., (2018). In contrast to the first set of simulations, the power grid was modeled according to the planned 2025 grid extension, see Figure 13, and we allowed considered a matrix of plant configurations with power ratings from 100 MW to 500 MW (in 100 MW increments) and capacities from 100 MWh and 500 MWh (in 100 MWh increments). The goal was to obtain a first indication of how the plant size, as characterized by its power and capacity, affected a net system profit. This quantity was defined as the difference in energy production costs with and without the AA-CAES plant minus the plant construction and maintenance costs. The plant cost model was derived from that presented by Motmans (2017). The plant was assumed to have an efficiency of 70%.

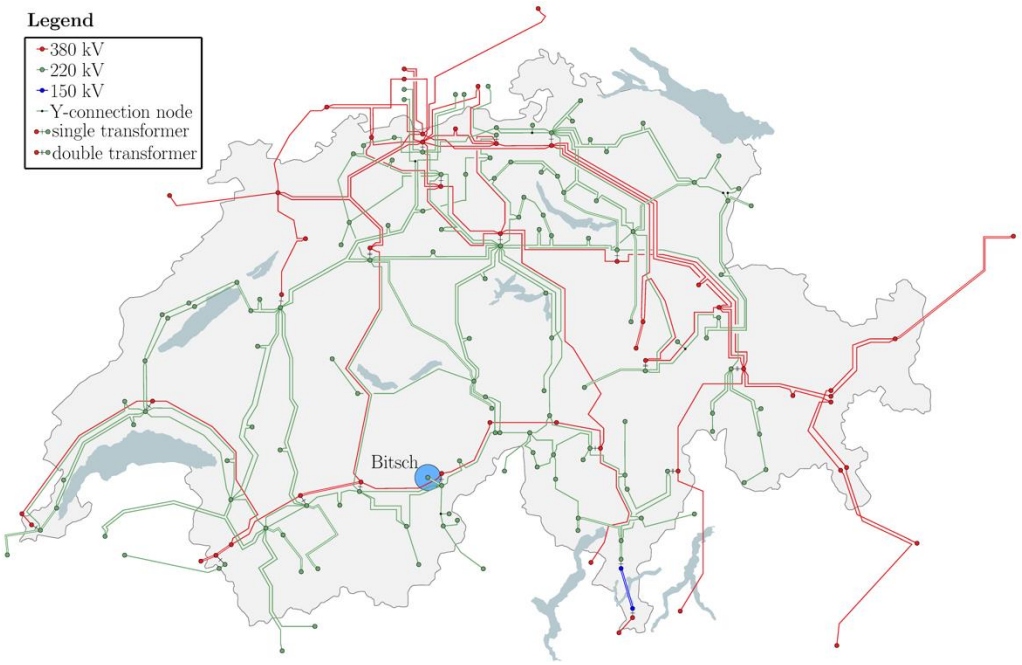


**Figure 13: Power-grid representation in second set of simulations.**

The results of the simulations for the use case of arbitrage are shown in Figure 14 and make clear that arbitrage is not profitable irrespective of the plant power rating and capacity, see Ref. [8]. This result is consistent with prior estimates by ALACAES and the well-known difficulties of Swiss PHS plants operating with arbitrage.

Current work, performed within the framework of the SCCER HaE AA-CAES project, focuses on identifying alternative use cases in conjunction with BKW. In addition, we are incorporating a simplified model of the unsteady operation of the AA-CAES plant, derived from the interaction with MAN Energy Solutions Schweiz AG in this project, that includes the energy consumption during transient and idle periods in order to get more accurate estimates of the plant profitability. We anticipate using these results to study selected configurations using the detailed plant model described in this report to check whether the assumed plant efficiencies can be attained during unsteady operations.

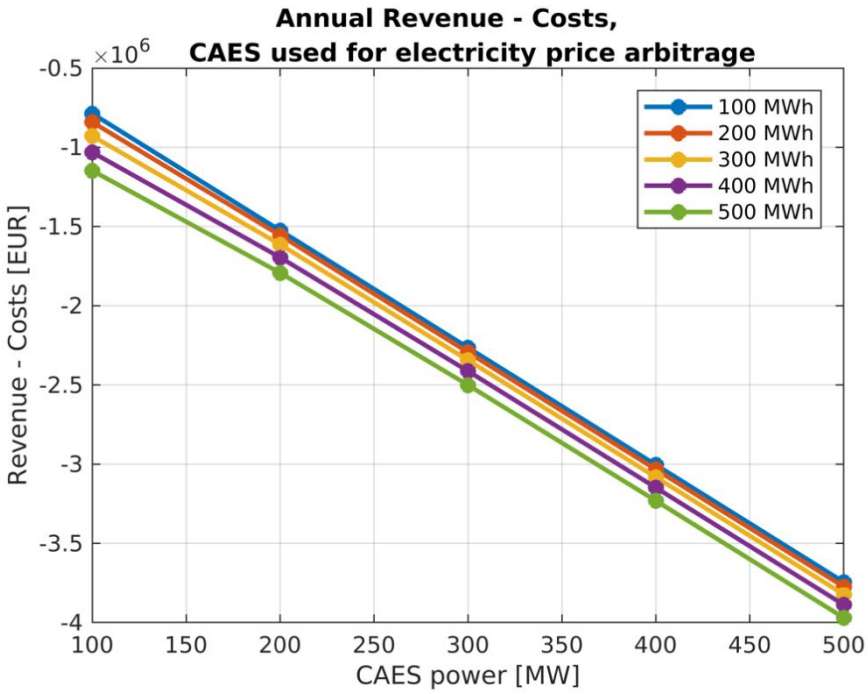


**Figure 14: Difference between revenue and plant construction and maintenance costs as a function of plant power rating and capacity, assuming the plant is located at the grid node near Bitsch, see Figure 13.**

# 4 AA-CAES turbomachinery

## 4.1 Summary of MAN-ES contribution into the AA-CAES project study

The MAN-ES contribution to the project has been focused on guidance regarding technical feasibility and cost-effective design of the turbomachinery units, which are one of the key components of the AA-CAES system. The support and contribution to the team can be summarized under the following main tasks or topics:

a) Definition of possible process topologies of the plant for an optimal integration of the turbomachinery, in terms of performance and cost.
b) Design layout and performance calculation of the compressor and turbine units for the integration into the plant model developed by SUPSI.
c) Technical process requirements, limitations and estimation of the transient operation of the compressor and turbine units (i.e. starting-up procedure).
d) Analysis of the transient behavior of the compressor and turbine units in order to reach the shortest achievable starting-up and shut-down periods as well as the related energy consumption during these transitory phases
e) Estimation of budgetary costs for the proposed compressor and turbine package (i.e. complete train including motors resp. generator)
f) Conceptual pre-analysis study of a combined compressor-expander machine feasibility.

MAN-ES has discussed together with the project team the general possible topologies, i.e., layout of the process suitable for an optimal integration into AA-CAES large scale commercial plants. MAN-ES has proposed a symmetric design of the temperature profiles in two stages, a low-pressure (LP) and a high-pressure (HP) stage. This results in similar temperature profiles for the LP and HP components (compressors, turbines, TES, piping, instrumentation, etc.). This design has been adopted for the present study.

For the two compression stages proposed, a detailed compressor layout has been performed, resulting in a choice of available but optimized turbo-compressors. For these compressors, the so called performance maps have been established displaying efficiency, power input, discharge temperature and suction capacity for all allowable operating points.

This data, transformed into a suitable numerical format, was successfully implemented by SUPSI into the plant model. The layout also comprises a control mechanism to achieve part load operation i.e. operating conditions at reduced mass flow and power input.

The requirements for the start-up procedure have been exchanged with the project team and a quantification of the overall start-up energy as well as start-up time has been elaborated.

On the turbine side, several layouts have been presented for the HP and LP turbines. Our common view on the requirements for these components has evolved during the project, focusing on the part-load operation of the turbines. Severe part-load operation presents a considerable challenge to maintaining high efficiency of the overall system. That is the reason why several iterative discussions and clarifications have been pursued in order to come to an acceptable level of detail required for this study.

Budgetary calculation of the costs for both proposed compressor and expander solution has been set up and provided to the project team. In addition, cost functions valid for similar turbomachinery components of different sizes (i.e., power) have been set up in order to estimate the cost by scaling-up or scaling-down the AA-CAES plant.

Finally, a first order feasibility and conceptual research study for a combined compressor and turbine machine applicable to the AA-CAES conditions has been achieved and presented to the project team.

## 4.2 Compressor selection and performance maps

The compressor units selected and optimized for the charging process of the AA-CAES study fit the high power requirement and relatively high pressure ratio (and outlet temperature) imposed by the AA-CAES charging process conditions (refer to the specification in Chapter 1). That's the reason why the compression duty from atmospheric inlet conditions to cavern pressure outlet conditions has to be split into two separate sections, i.e., two separate turbomachinery units, namely the so-called LP- and the HP-compressor. The LPC has been selected amongst the biggest available axial compressors of the MAN-ES portfolio, due to the high flow and high inlet volume flow requirement imposed by the AA-CAES process. The HPC has been selected amongst the biggest available radial compressors of the MAN-ES portfolio due to the relatively high outlet pressure and temperature imposed by the AA-CAES process. Typical informative pictures of the LPC and HPC units are shown in Figure 15.

**Figure 15: Examples of LP-compressor (left picture) and HP-compressor (right picture) suitable for the AA-CAES charging process**

The compressors are optimized for a single design point of operation specified to be the nominal operating condition of the AA-CAES charging process and with the maximum achievable thermodynamic efficiency. In addition, the variable inlet geometry (called "inlet guide vanes") allows the operation and control of the LPC and HPC in a broad range of operating conditions (i.e., variable mass flow rates, power and outlet pressure). The operating and performance data of both LPC and HPC can be predicted and visualized in the so-called performance maps, i.e., power and discharge pressure versus mass flow rate for various inlet geometry angle position. The set of performance prediction data in the whole operating range of the LPC and HPC was forwarded to SUPSI and has been implemented in the AA-CAES plant model.

## 4.3 Turbine selection and performance maps

The turbine units selected and optimized for the discharging process of the AA-CAES study fit the high power requirement and relatively high pressure ratio imposed by the AA-CAES discharging process conditions (refer to the specification in Chapter 1). The HPT and LPT selected for this study are axial turbine types in order to absorb the high volume flow imposed by the AA-CAES process conditions. In addition, axial turbine types lead generally to better performance (i.e., thermodynamic efficiency) than radial models. That's why they were chosen and optimized to deliver the best achievable efficiency over a broad range of operation. The HPT was designed to be a single flow axial turbine and the LPT

a double flow axial turbine, in which the high volume flow is split into two symmetrical sections. Typical informative pictures of the LPT and HPT train are shown in Figure 16.

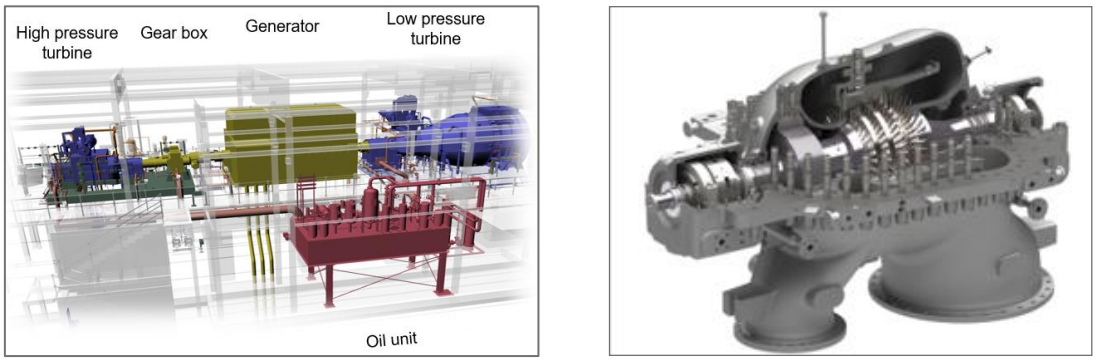


**Figure 16: Examples of the HP+LP turbine train (left picture) and typical radial turbine layout (right picture)**

The two turbines were designed in a way that the intermediate pressure between the LPT and the HPT turbine match the specified requirement imposed by the cavern intermediate pressure, as explained in Chapter 1). Hence, the LPT is a so called “sliding pressure” turbine design. This means that the inlet pressure of the LPT is a function of its operating condition since the outlet conditions are fixed to the atmospheric conditions. The HPT is designed so that it can cope with the various inlet pressures occurring in the cavern. A variable valve opening system controls the flow entering in the machine. Once the valve is completely open, a bypass and re-injections manifold system helps controlling a safe and flexible operating range (i.e. variable pressure, flow rates thus power generation). The operating and performance data of both LPT and HPT in the possible range of operation were generated in numerical format only, forwarded to SUPSI and have finally been implemented in the AA-CAES plant model.

## 4.4 Transient turbomachinery behavior

The transient turbomachinery behavior is an important element to be considered for the assessment of the AA-CAES plant performance and profitability. In particular the turbomachinery transient behavior during the start-up and shut-down phase of the plant need to be considered. In addition, also the energy consumption of the turbomachinery between the charging and discharging phase, i.e., during the idle period, may have a relevant impact on the profitability.

### *Compressors*

The transient compressor behavior has been assessed for a compression train with a nominal power of 140 MW (75 MW axial and 65 MW radial). This corresponds to a mass flow going into the cavern of approximately 200 kg/s. A change in compressor design power has an important impact on the transient behavior, start-up and shut-down times. Three different modes between two plant charging events are possible: hot, warm and cold.

In hot mode the compressor train is electrically synchronized with the grid and therefore rotating at 3000 rpm (50Hz grid frequency). The minimum power required to keep the compressor in this mode is

considerable, because the compressor has to process a minimum amount of air to avoid surge. The energy spent to keep the compressor in this mode is mainly lost. Hence, this operating mode is only attractive for very short periods during two charging events. On the other hand the time required to reach maximum power is much faster because the compressor train is already at nominal speed.

In warm mode, the compressor casing and the rotating parts are kept at a sufficiently high temperature that allows immediate ramp up to nominal speed (3000 rpm). If the compressor is not kept at a certain temperature, thermal transient effects would cause collision between the rotating and stationary parts. Similar effects require that the compressor is kept in so called slow-roll mode during the first days after run down. In this mode the compressor is rotating at very low speed to avoid bending of the rotor caused by thermal transients. The energy consumption during this phase is considerably lower compared to the synchronized hot mode and is mainly caused by the oil systems, slow-roll motor and heating systems. However, the start-up time is longer from the warm phase as the train has first to be brought up to nominal speed. The energy required for the ramp-up of the compressor train to nominal speed is much smaller compared to the energy required to bring the compressor from idle power to maximum power when already at nominal rotating speed. Depending on the cavern pressure and desired charging power, up to 90% of this energy can be considered as stored energy in the cavern.

In cold mode, all systems are switched off and the compressor is at stand-still and at ambient temperature. The start-up of the compressor is much longer as the oil needs to be heated up first, for instance. It is expected that his mode only makes sense for very long shut-down times of several days or weeks. In general, the choice of the compressor operating mode (hot, warm, or cold) between two charging cycles is an outcome of the simulations and optimizations.

***Turbines***

The transient turbine behavior has been assessed for an expansion train with a nominal power of 100 MW (50 MW high pressure and 50 MW low pressure with re-heat between the two turbines). A change in turbine design power has an important impact on the transient behavior, start-up and shut-down times. The same three different operating modes between two plant discharging events are considered for the turbines as well: hot, warm and cold.

In hot mode, the turbine train is electrically synchronized with the grid and therefore rotating at 3000 rpm (50 Hz grid frequency). In this mode, a minimum power output of a few percent of the nominal power is necessary, resulting in a slow discharge of the energy stored in the TES and in the cavern. This minimum power has to be absorbed by the grid or must be used for other purposes. If this energy cannot be used, this operating mode is only attractive for very short periods during two discharging events. As for the compressor, the time required to reach maximum power is significantly faster because there no ramp-up and synchronization with the grid are required.

In warm mode, the turbine casing and the rotating parts are kept at a sufficiently high temperature that allows immediate ramp up to nominal speed (3000 rpm). Similar to the compressor, a certain temperature level is required to avoid collision between rotating and stationary parts caused by thermal transient effects. Similar effects require that the turbine is kept in so-called rotor turning gear during the first days after run down. In this mode, the turbine is rotating at very low speed to avoid bending of the rotor caused by thermal transients. In warm mode, there is no power output and storage discharge, but this operating mode requires a relatively small energy consumption mainly caused by the oil-systems, slow-roll motor, and heating systems. Furthermore, the start-up time is much longer from the warm phase as the train has first to be brought up to nominal speed and then needs to be synchronized to the grid, before the power production and ramp-up to maximum power can start. The energy required during speed-up of the turbine train is not very large, but has to come from the storage and is lost.

In cold mode all systems are switched off and the turbine is at stand-still and ambient temperature. The start-up of the turbine from cold conditions is much longer. First the oil and the casing need to be heated up. Secondly and different compared to the compressors, the ramp-up to maximum power, after the turbine has been brought up to nominal speed and after synchronization, takes much longer compared to the warm operating mode. Like for the compressor, it is expected that his mode only makes sense for very long shut-down times of several days or weeks.

Generally speaking, the warm operating mode of the turbomachines between two charging or discharging cycles seems to be the most attractive option, unless short response times of a few seconds are required and the corresponding loss of energy is within the profitability targets. The energy requirements for keeping the turbines and compressors in the warm mode are relatively low and are expected to predominate the long start-up times from cold mode. Finally, the choice of the compressor and turbine operating modes (hot, warm or cold) between two charging or discharging cycles is an outcome of the simulations and optimizations.

## 4.5 Compressor-Expander machine concept

A separate topic about the combination of compression and expansion stages in one single machine has been discussed with the project team.

Combining the compression and the expansion process in one single solution can basically be done as:

a) Integration of dedicated stages for compression and expansion attached to one single driver/generator. This can be done in one common or separate, individual casings.

b) Use of the same stages for both, compression and expansion.

Both concepts have their advantages and disadvantages. The second concept is particularly challenging as the flow physics are fundamentally different in a turbo machine that builds up pressure compared to a pressure drop in the direction of the flow. For this reason, the existing turbomachinery looks quite different for compressors and turbines of comparable volume flow and pressure ratio.

**Integration of dedicated stages in one train or casing**

1.) Example Huntorf train [12]. Several casings with one driver/generator. Challenges involve the complicated clutch required (e.g. Synchro-self-shifting clutch used here), the very long trains limiting the operational flexibility and eventually the complexity and reliability.

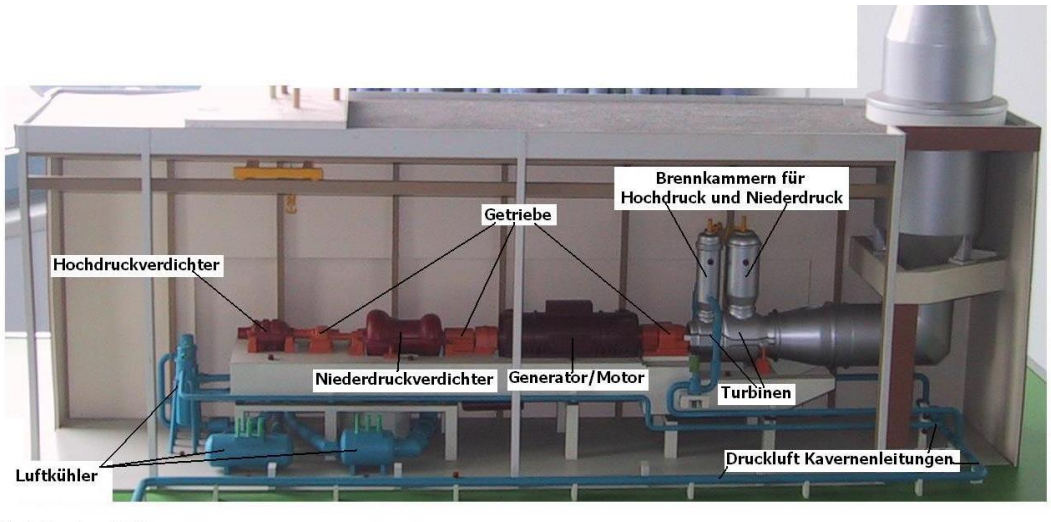


**Figure 17: Huntorf compression/expansion train.**

2.) Multi stage gear type radial compressor and expander. Some stages are compression stages, some are expanding stages, all stages are connected to the central bull gear. The challenge is to determine what the compression stage is doing while the overall process is expanding and vice versa.
Radial turbomachinery is less efficient and more expensive than axial turbomachinery at high volume flow and high power (> 50 MW). Technology not yet available for all options.

**Figure 18: Multi stage gear type radial compressor and expander.**

**Same stage for both, compression and expansion**

1.) A volumetric piston compressor can also be used as an expansion machine, then requiring active valve control.
Volumetric piston compressors are typically used to achieve very high pressures at low volume flow, which appears, by trend, opposite for the AA-CAES application. Hence, cost effective scalability to very large scales of energy storage plants seems very questionable

at this stage. Pressure pulsations are experienced in the process media. When considering other volumetric compressors, the technical challenges encountered are similar to those for piston compressors.

2.) Turbomachinery with compression and expansion in the same stage/impeller.

- Wells turbine, in commercial operation for wave power stations. Operation as turbine with bidirectional airflow is possible without changing the sense of rotation thanks to the symmetric airfoils (see Figure 19). This system would have to be modified for compression purpose, but is claimed to have low efficiency. Further problem is the low rotation speed to avoid blades stall.

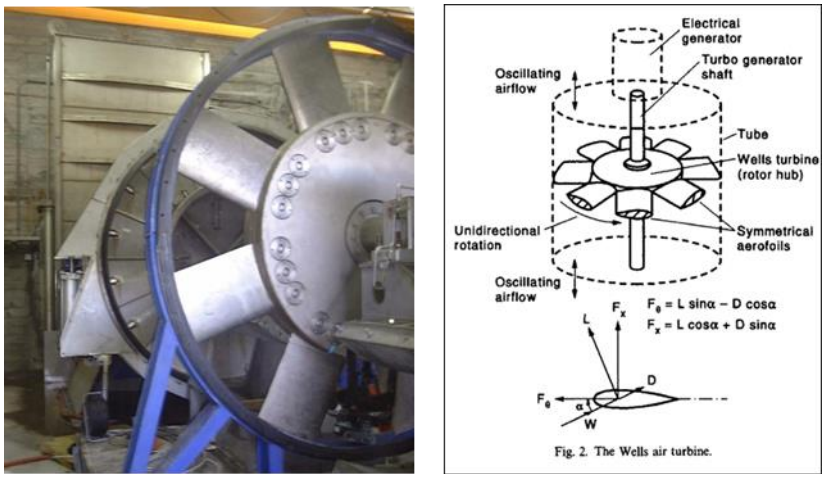


**Figure 19: Wells turbine.**

- A turbine with radial inlet and outlet rotor for use in bidirectional flows is presented in the US Patent N. 2013/0011251 A1. No industrial application is known. It is not clear if modification for compression purpose would be possible.

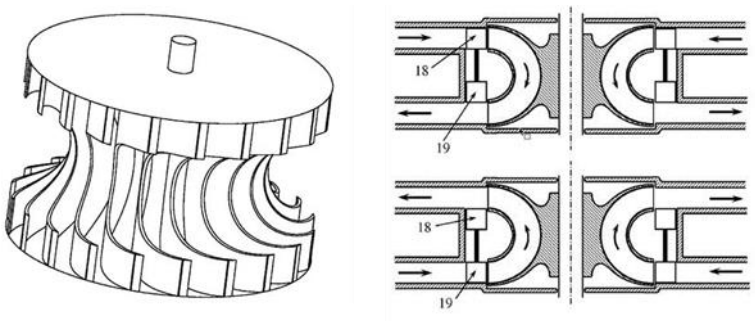


**Figure 20: Combined machine from US Patent 2013/0011251 A1.**

- A cooperation between Fraunhofer UMSICHT and BOGE Kolben-Kompressoren was established for CAES technology. A development project was claimed and the plant configuration is unpublished yet. The partnership declares that the same

machines can be used for compression and expansion, by combination of a turbomachine with a piston machine [13].

- Use of radial compressor stages also for expansion. Basic research is required, no industrial application is known. Requires a different sense of rotation for compression and expansion. Pressure ratio per stage probably limited by the compression purpose. Average efficiency for compression plus expansion is seen as challenge.

Most of these solutions operate at low power, pressure and temperature. Important challenges may come from transferring them to a larger scale. Their practical applicability, efficiency, power density and part-load behavior remain unknown at the time being.

# 5 Thermal-energy storage

The thermal-energy storage (TES) was not a major focus of the AA-CAES-G2G project. Nevertheless, some of the recent results achieved as part of the SCCER HaE AA-CAES project, see Ref. [11], are briefly described here because of the close relationship between the SCCER HaE and SFOE G2G projects.

Because the operating profile of AA-CAES plants is governed by future electricity markets and therefore dynamic, the TES must also be able to deal with dynamic operating conditions. Thermocline TES with rocks as storage media are particularly attractive for AA-CAES plants because they are well suited to air as the working fluid and because of their simple construction. Now it is known that thermocline TES can require up to 50 cycles to return to their nominal quasi-steady-state behaviour following a disturbance in their operating schedule. TES systems that consist of multiple smaller storage units and that can be used in combination, appear to be better suited to off-design operation, see [8]. There are at least three additional potential benefits to considering such so-called multi-tank TES systems for AA-CAES:

1. If the cavern is excavated as a constant-diameter tunnel, a single TES tank with circular cross section may not fit within the tunnel. An alternative would be to consider tanks with rectangular cross sections as in the pilot plant. However, this increases the surface-to-volume ratio and hence the thermal losses from the TES to the air in the cavern. Another alternative would be to increase the diameter of the cavern around the location of the TES, but this would increase the cost of constructing the cavern, especially when it is equipped with a lining to reduce pressure losses.

2. Multi-tank TES systems represent a simple way to implement thermocline control (TCC), which was shown to be an effective way to greatly increase utilization factors with small penalties in exergy efficiency, see [6] and [7] The mixing TCC method even allows the TES outflow temperature – and hence the turbine inflow temperature − to adhere to specified minimum values.

3. A third benefit, closely related to the second, is that the mixing TCC method can in principle be used not just to keep the TES outflow temperature constant, but to keep the turbine power output constant, which is anticipated to be beneficial for grid operation.

# 6 Model results

The AA-CAES numerical model was firstly exploited to evaluate the performance of a full scale plant (cavern operating pressure up to 100 bar) with the turbomachinery selected by MAN ES. After that, two smaller plants, whose maximum cavern pressures were 80 and 60 bar respectively, were also simulated. This chapter presents the details of the simulations of these plants
Furthermore, an analysis about the plant performance sensitivity to air properties and the effect of the AA-CAES plant schedule are presented.

## 6.1 Full scale AA-CAES plant: 100 bar

A full-scale AA-CAES plant was simulated when operating with a scheduling composed by a pre-charge and a series of 50 identical cycles composed of 5 hours of charge and 5 hours of discharge, including 0.1 hour of idle between them. The mechanical efficiencies of electric motor and generator were set to 0.98. The cavern had a volume of 177'000 $m^3$ and a wall area of 18'150 $m^2$. Both the LP and HP TES had a reverse truncated cone shape, a height of 15 m, a top diameter of 32 m and a bottom one of 24.5 m. They were both assumed adiabatic. The TES chamber dimensions were assumed 34 x 34 x 16 m in order to accommodate the LP TES. Thermal losses of the cavern and the TES chamber were modelled with a constant convective heat-transfer coefficient of 20 $W/m^2K$.

The total power adsorbed by the plant during the charging phases was set to 140 MW. TES chamber pressure was controlled regulating the HP compressor during charging phases while it was "sliding" during discharging phases. The outlet temperature of the intercooler before the HP compressor was set to 20°C while the maximum outlet temperature of the intercooler after the HP turbine to 200°C.

Figure 21 depicts the simulated efficiency of the plant, which is around 75% including the energy required for turbomachinery transients and stops. Figure 22 depicts the power of each turbomachine during the last three cycles. Due to the sliding pressure condition, during a discharge phase, the turbine train power output decreases 10.5 % from roughly 114.4 MW to 102.4 MW. Pressure and temperature variation in the cavern and in the TES chamber can be seen in Figure 23 and Figure 24 respectively.

Figure 25 to Figure 28 show the LP and HP TES thermoclines evolution after charge and discharge along the entire sequence of cycles. From these figures, we notice that both TESs reached stable operating conditions (successive thermoclines, after a certain number of cycles, are superimposed). The large temperature difference at the top of the HP TES was caused by the sliding operation of the HPC.

The operating points followed by the turbomachinery during the simulation are reported in Figure 29 to Figure 32: these points fall into normal operating regions of the efficiency maps for the largest part of turbomachinery operation time (>96%).

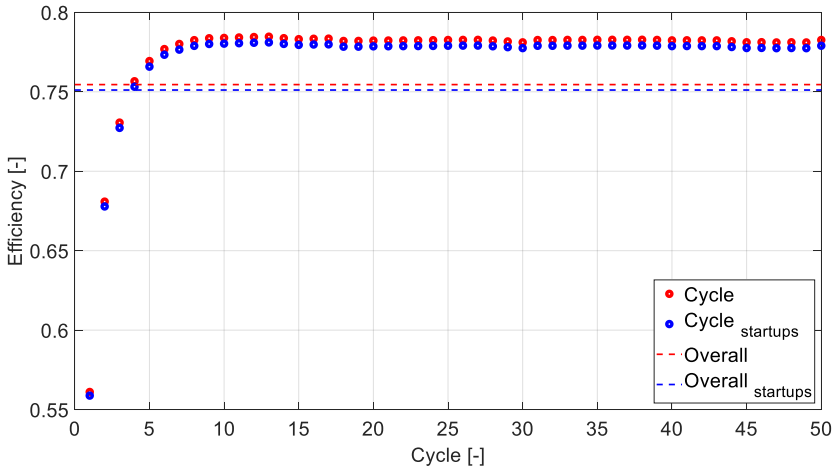


**Figure 21: Efficiencies of AA-CAES plant, maximum pressure of 100 bar.**

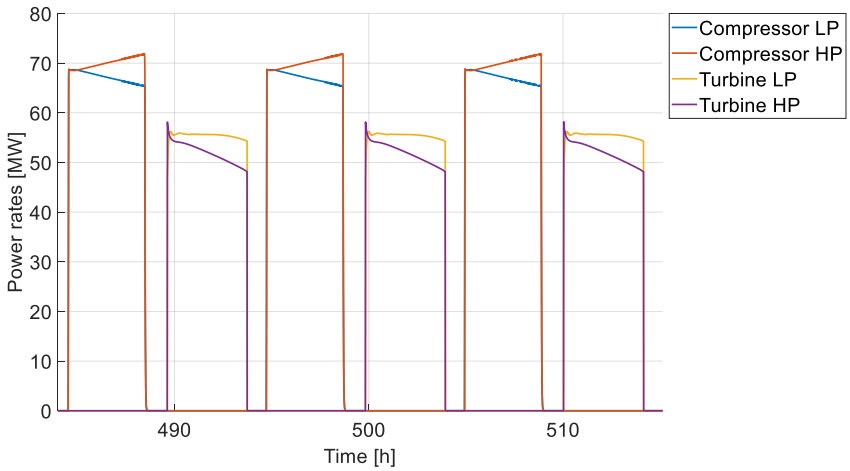


**Figure 22: Turbomachinery power during the last 3 cycles.**

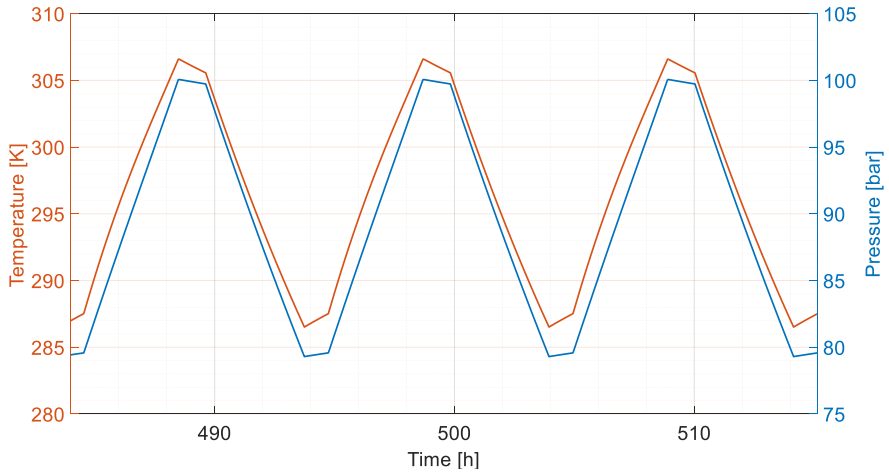


**Figure 23: Temperature and pressure in the cavern during the last 3 cycles.**

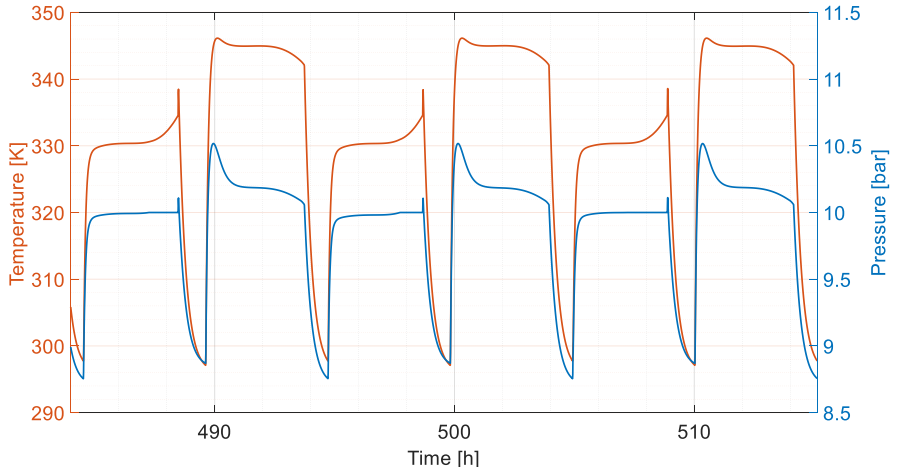


**Figure 24: Temperature and pressure in the TES chamber during the last 3 cycles.**

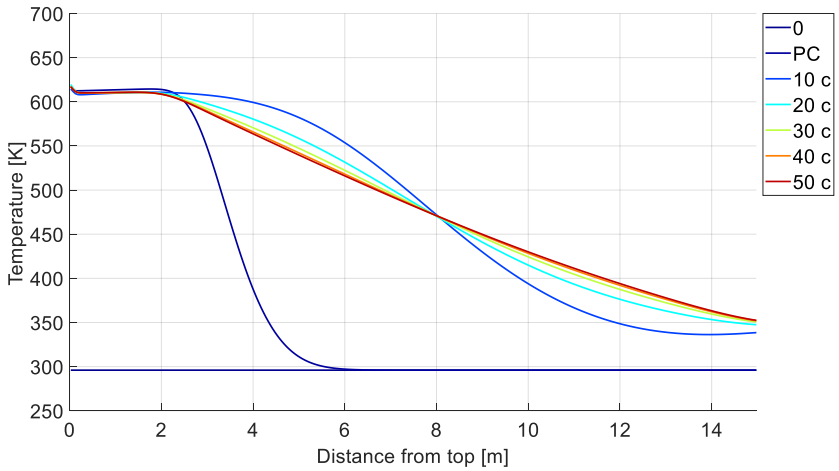


**Figure 25: Thermoclines at the end of the charge phases, LP TES.**

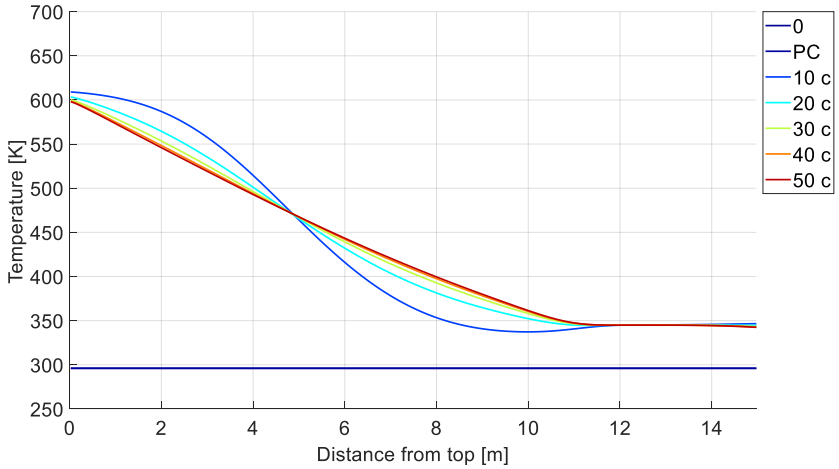


**Figure 26: Thermoclines at the end of the discharge phases, LP TES.**

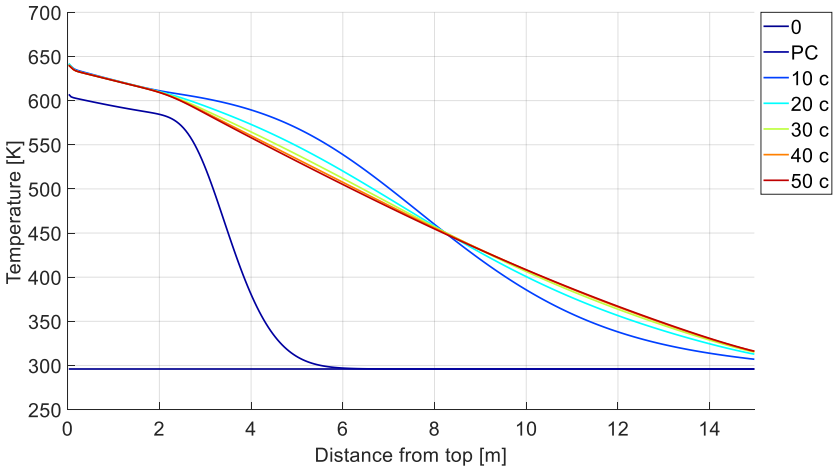


**Figure 27: Thermoclines at the end of the charge phases, HP TES.**

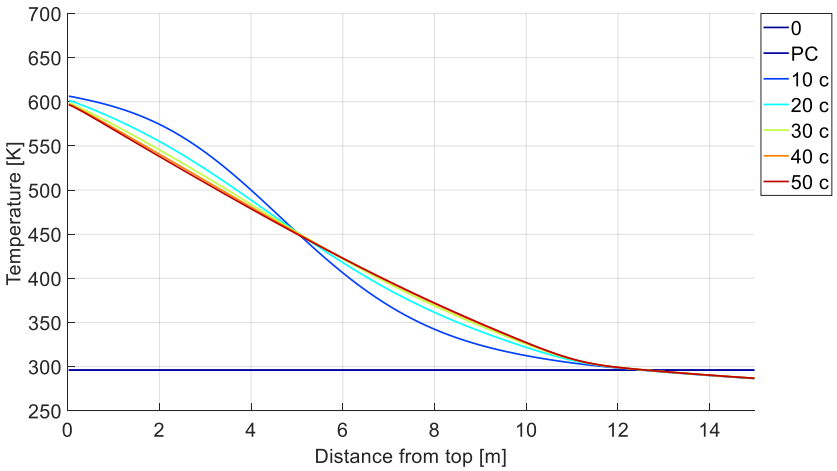


**Figure 28: Thermoclines at the end of the discharge phases, HP TES.**

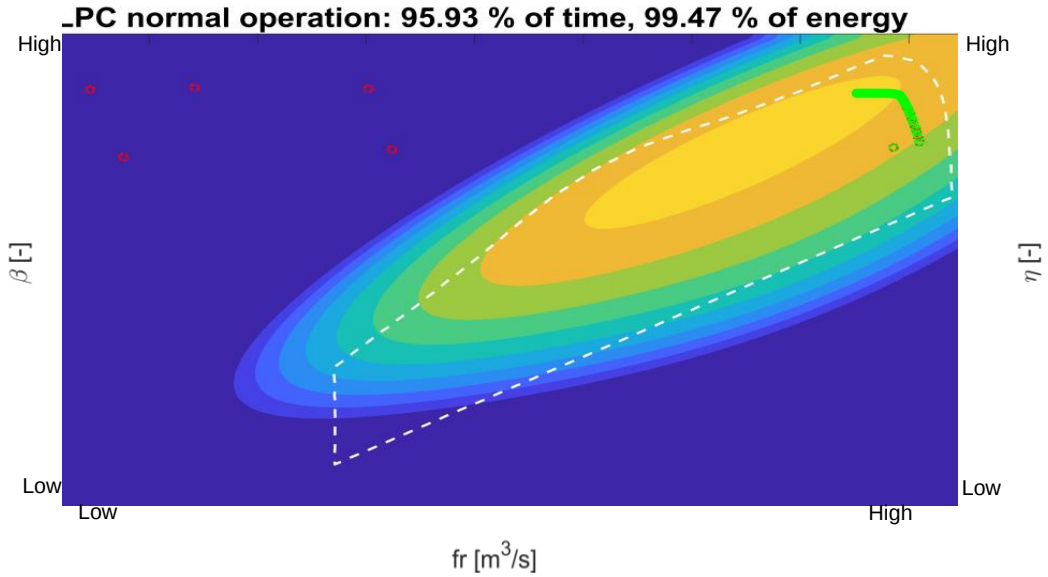


**Figure 29: Operating points of the LPC during the last cycle superimposed on efficiency contour. Red circles are outside the normal operating region, green ones are inside.**

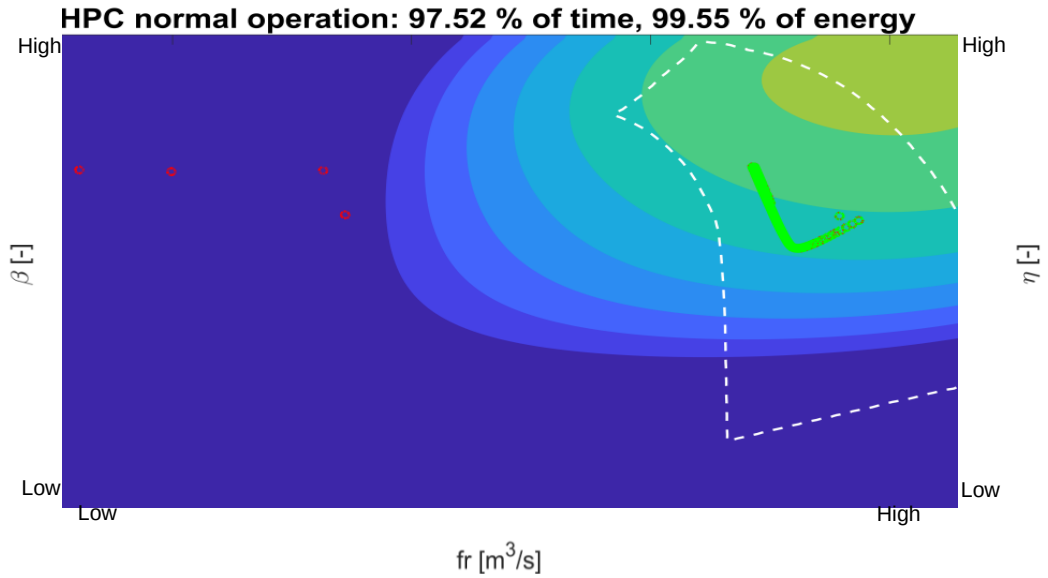


**Figure 30: Operating points of the HPC during the last cycle superimposed on efficiency contour. Red circles are outside the normal operating region, green ones are inside.**

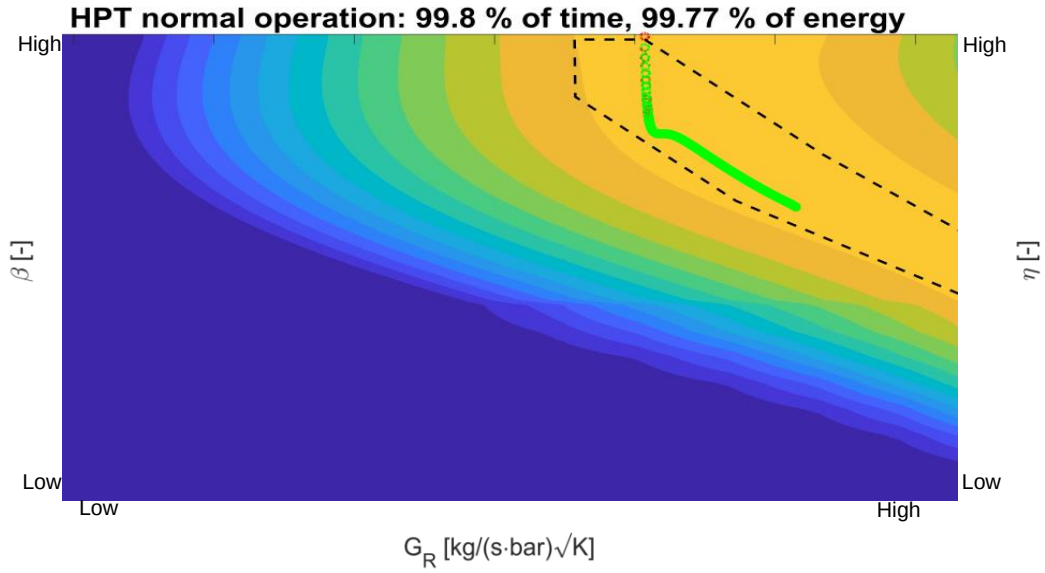


**Figure 31: Operating points of the HPT during the last cycle superimposed on efficiency contour. Red circles are outside the normal operating region, green ones are inside.**

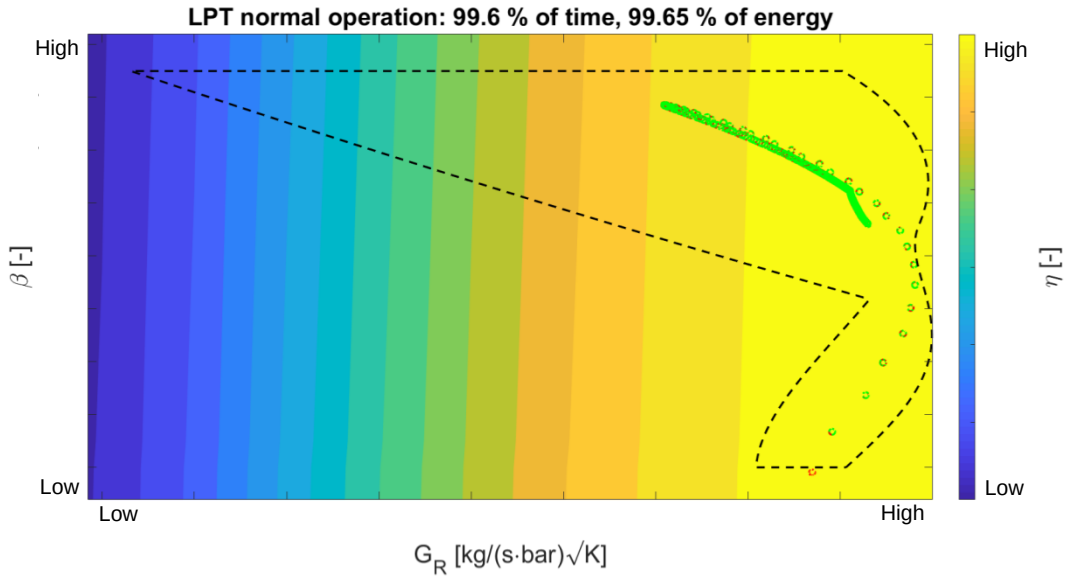


**Figure 32: Operating points of the LPT during the last cycle superimposed on efficiency contour. Red circles are outside the normal operating region, green ones are inside.**

## 6.2 Turbomachinery downscaling

Different sizes of the same plant configuration were studied to verify how the plant efficiency would be affected. Two downsized plants were considered characterized by two maximum pressure level in the cavern, 80 and 60 bar.

### 6.2.1 Turbomachinery start-up

The energy requirements for the transients and idle phases described for the original plant size were kept unchanged for the downscaled AA-CAES layouts, in a conservative assumption.

### 6.2.2 Turbomachinery: performance maps

In order to match the different pressure levels in both the cavern and the TES chamber, some adaptations of the turbomachinery were necessary: the air compression was obtained dividing evenly the overall compression ratio among the LPC and HPC. Furthermore, Table 5 summaries the factors used to modify the efficiency maps of the turbomachinery: following the directives of MAN ES, performance maps of downscaled compressors were obtained preserving volumetric flow rates while compression ratios were reduced to fit the new pressure ranges.
The same approach was used for the turbines. Specifically, for them, the relation correlating the mass flow rates to their inlet pressure had to be adjusted and therefore also the $G_R$ values, due to their dependence to the inlet pressure (see Eq. (12)).
The downsized plants have obviously different overall performance: power absorbed during charge is 110 MW for the 80 bar plant and 90 MW for the 60 bar plant.

**Table 5: Summary of the factors applied to downscale the turbomachinery maps and fit the AA-CAES layouts characterized by a maximum cavern pressure of 80 and 60 bar.**

| | | |
|---|---|---|
| $\beta_{80} = \beta \cdot 0.85$<br>$\beta_{60} = \beta \cdot 0.75$ | 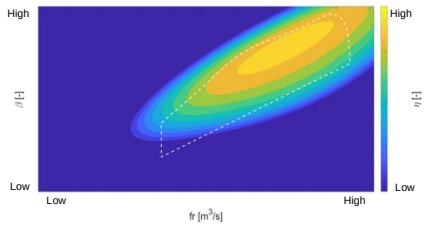 | $G_{R,80} = G_R/0.85$<br>$G_{R,60} = G_R/0.75$ |
| $\beta_{80} = \beta \cdot 0.90$<br>$\beta_{60} = \beta \cdot 0.85$ | 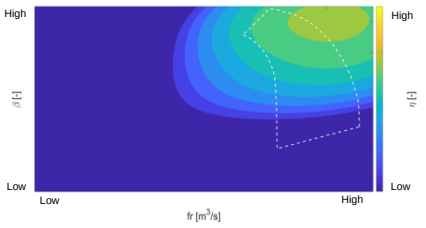 | $G_{R,80} = G_R/0.80$<br>$G_{R,60} = G_R/0.60$ |
| $\beta_{80} = \beta \cdot 0.85$<br>$\beta_{60} = \beta \cdot 0.70$ | 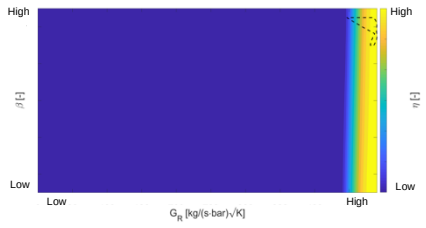 | |
| $\beta_{80} = \beta \cdot 0.90$<br>$\beta_{60} = \beta \cdot 0.80$ | 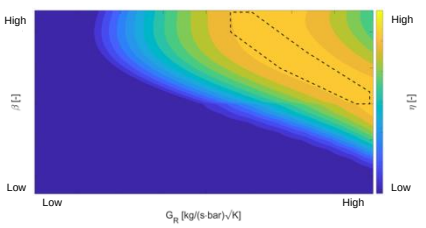 | |

### 6.2.3 Results of downscaled AA-CAES plant: maximum pressure of 80 and 60 bar

The plant scheduling composed by a pre-charge and a series of 50 identical cycles composed of 5 hours of charge and 5 hours of discharge, including 0.1 hour of idle between them was performed in these cases also.

The dynamic interconnection of the plant components (cavern, TES chamber, turbomachinery) makes an AA-CAES plant more complex than a classical Brayton cycle with reheat. Therefore, it is important to verify that the plant dynamics is compliant with turbomachinery design data. The TES chamber pressure obtained in the plant simulations is always within the constraints of the LP turbine pressure inlet. It can be noticed that the three AA-CAES plant efficiencies, reported in Table 6, are very similar.

Table 7 summarizes turbomachinery power variations within a cycle: the component affected by the greatest variation is the HPT (around 20%, on average). On the other hand, there are no power variations in the compressor train since the total power is fixed. The effects of the increase of cavern pressure and variation of mass flow rate during the charge cycle can be seen by the fact that the LPC reduces the power (less mass flow rate at the end) whereas the HPC increases the power request due to the back pressure (cavern pressure) increase.

**Table 6:Plant overall efficiencies.**

| | $\eta$ [-] |
|---|---|
| **60** | 74.6 |
| **80** | 75.5 |
| **100** | 75.1 |

**Table 7: Turbomachinery powers and percentage variation during the last cycle.**

| | | LP [MW] | | | HP [MW] | | | Train [MW] | | |
|---|---|---|---|---|---|---|---|---|---|---|
| | | **start** | **end** | | **start** | **end** | | **start** | **end** | |
| **Compressor** | **60** | 41.25 | 38.66 | -6.28% | 47.03 | 49.54 | 5.34% | 88.28 | 88.20 | -0.09% |
| | **80** | 51.16 | 48.61 | -4.98% | 56.65 | 59.29 | 4.66% | 107.81 | 107.9 | 0.08% |
| | **100** | 68.68 | 65.47 | -4.67% | 68.52 | 71.89 | 4.92% | 137.20 | 137.36 | 0.12% |
| **Turbine** | **60** | 43.77 | 40.52 | -7.43% | 52.18 | 38.48 | -26.26% | 95.95 | 79.00 | -17.67% |
| | **80** | 49.74 | 45.84 | -7.84% | 57.10 | 45.19 | -20.86% | 106.84 | 91.03 | -14.80% |
| | **100** | 56.20 | 54.27 | -3.43% | 58.20 | 48.12 | -17.32% | 114.40 | 102.39 | -10.50% |

In the following, Figure 33 to Figure 45 report each specific results of the three plants in single a page so to make the comparison easier.

Figure 33 depicts the cycle efficiency of the AA-CAES plants excluding and including the energy of transients and that required during compressors and turbines stops. The influence of these losses on the overall efficiency, for the given cycle, is actually limited and their relative effect do not change with the plant size.

Turbomachinery power is plotted in Figure 34: during the charges a constant power of 140 MW, 110 MW and 90 MW (plant target values) was absorbed by the compressor trains. During discharges instead, the power released by the plant depended, as stated above, on the caverns and TESs evolutions. The HPT stage was the one characterized by the higher power variation within a cycle, mainly due to the pressure variation at inlet. This aspect is further amplified reducing the power of the plant.

Figure 35 shows the thermal power extracted by the heat exchangers: as expected, the only active component was the one before the HPC. The intercooler was essential to preserve this machine, since the TES chamber air temperature increases cycle after cycle due to the air discharged by the HP turbine, which furtherly heats up the bottom layers of the LP TES.

Figure 36 and Figure 37 illustrate the temperature and pressure in the main cavern and in the TES chamber, respectively. While the pressure difference between the maximum and minimum one in the cavern is the same for all the configurations (20 bar), the temperature difference experienced by the air stored in the cavern increased as the pressure decreased. This can be justified by the fact that keeping the same cavern volume, a higher pressure translates into a higher density and therefore a higher mass stored within the cavern and a higher thermal capacity, which dumps down temperature oscillations. The drops of pressure visible in Figure 37 at the ends of charging and discharging phases were due to the air convective heat exchange with the TES chamber walls, which decrease the temperature and consequently the pressure.

From Figure 38 to Figure 41 the thermoclines within the LP and HP TESs after charges and discharges throughout the 50 cycles are reported. Again, both TESs reached stable operating conditions since the difference between thermoclines in the last 10 cycles are negligible.

Figure 42 and Figure 43 report the operating points of the LPC and HPC during the last cycle superimposed on efficiency contours. The white dashed line in both charts delimits the normal operating envelope of the machine. Red circles highlight those points outside the normal operating region, occurring during the power ramps at the beginning and end of operations, while green ones are those that represent normal operation.

Figure 44 and Figure 45 illustrate the operating points of the HPT and LPT during the last cycle superimposed on efficiency contours. Even though the LPT did not work completely inside the best operating region for the downscaled expanders, their operating points are very close to its boundaries and therefore were assumed as acceptable. Very few points are outside the normal operating region and the main cause for both the HPT and LPT are the thermal losses of the TES chamber, which cooled down the air and let the pressure drop, increasing the expansion ratio in the HPT and decreasing it in the LPT. These points are hence related just to the initial instants of the charging and discharging phases.

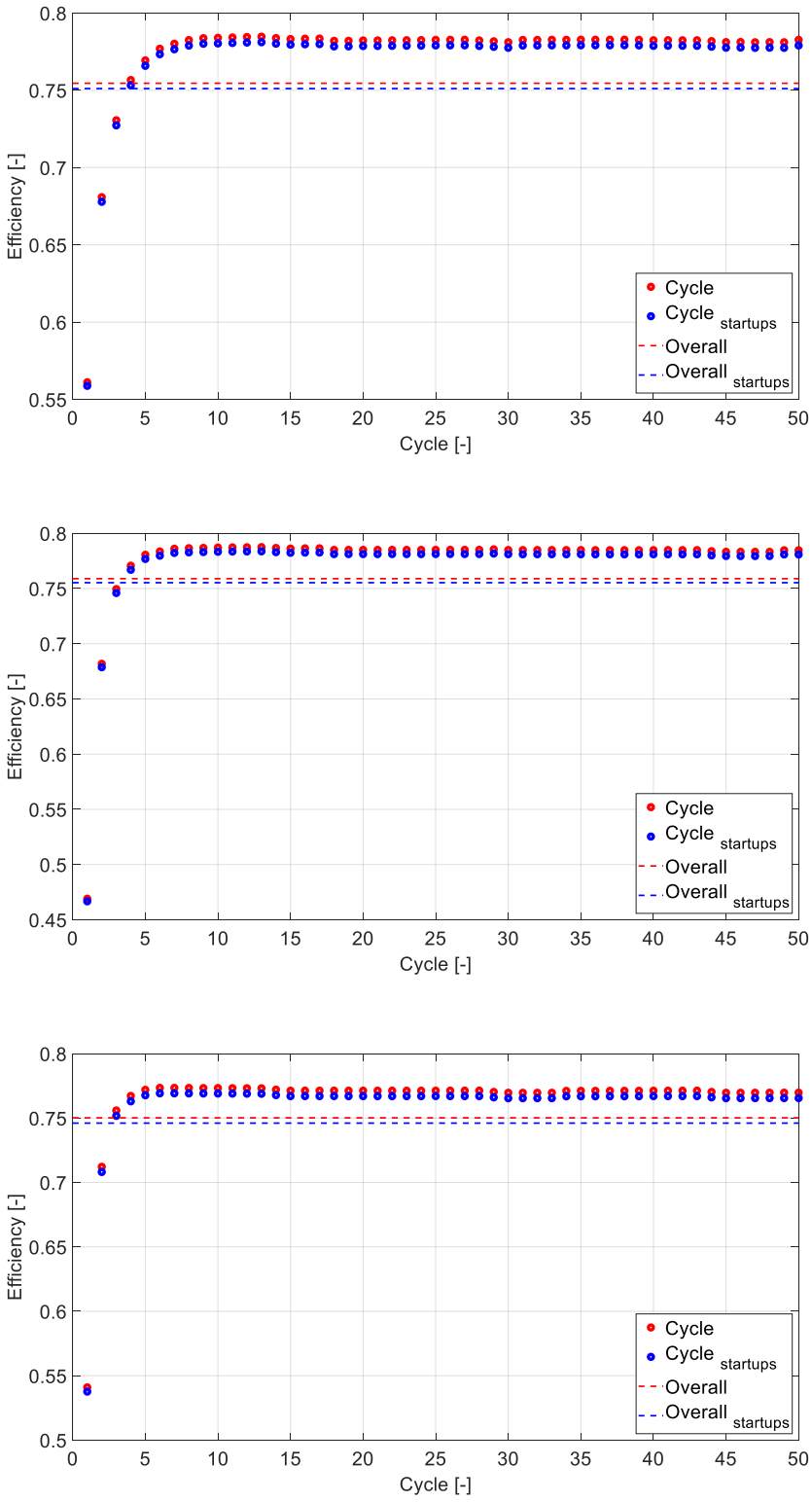


**Figure 33: Efficiencies of AA-CAES plant with different maximum pressures. From top to bottom: 100, 80 and 60 bar.**

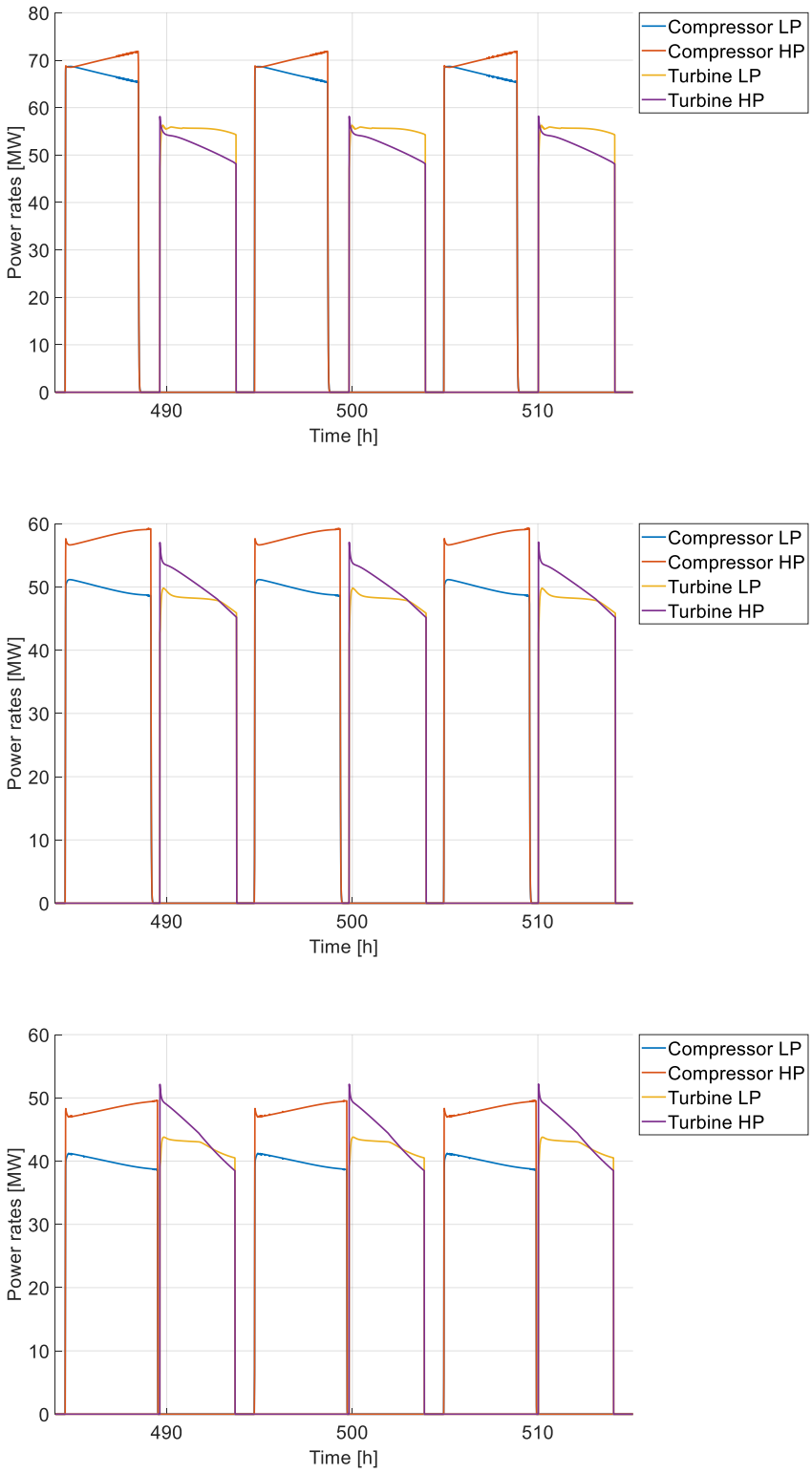


**Figure 34: Turbomachinery power during the last 3 cycles.**
**From top to bottom: maximum cavern pressure set at 100, 80 and 60 bar.**

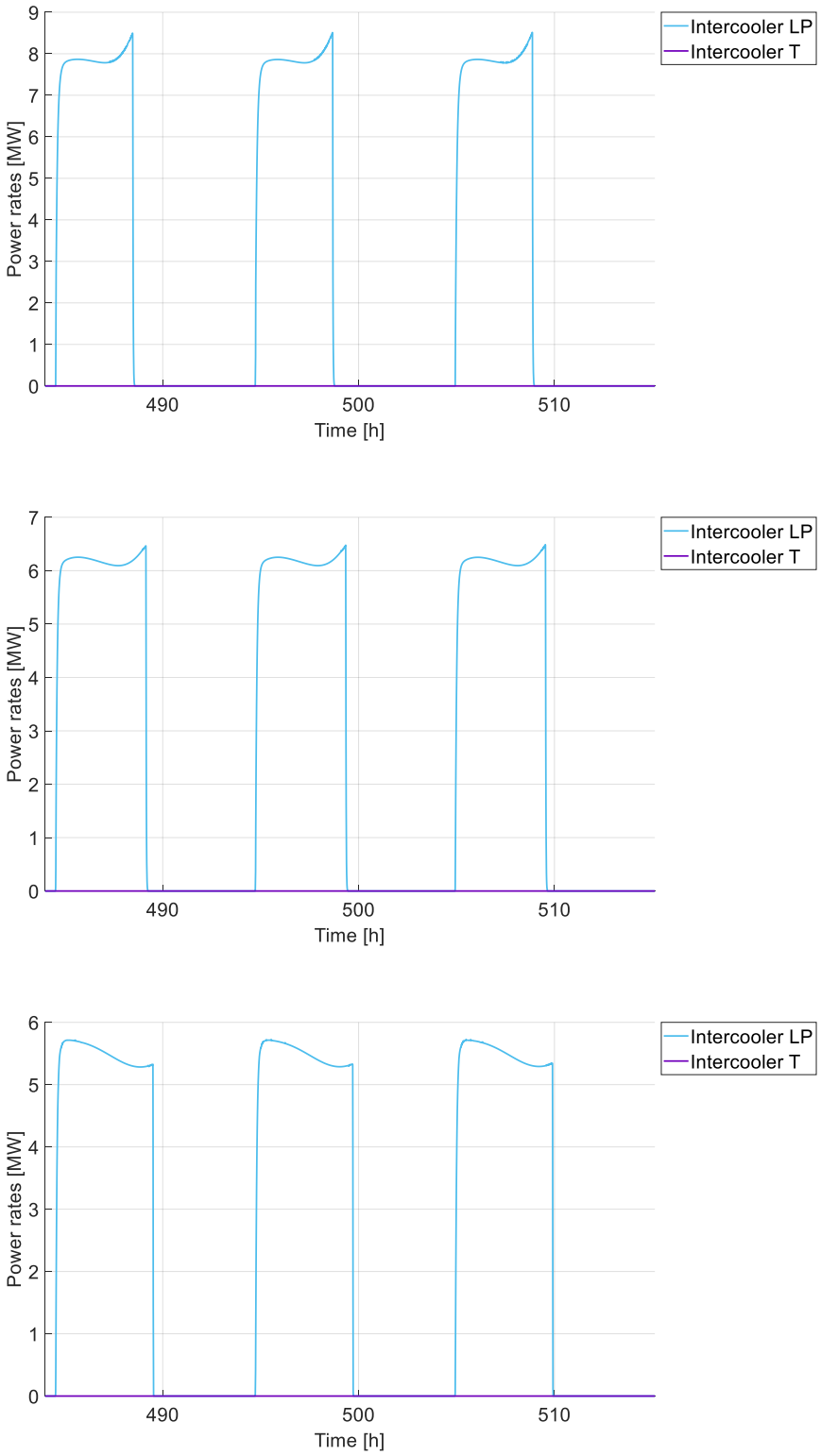


**Figure 35: Thermal power extracted from heat exchangers during the last 3 cycles. From top to bottom: maximum cavern pressure set at 100, 80 and 60 bar.**

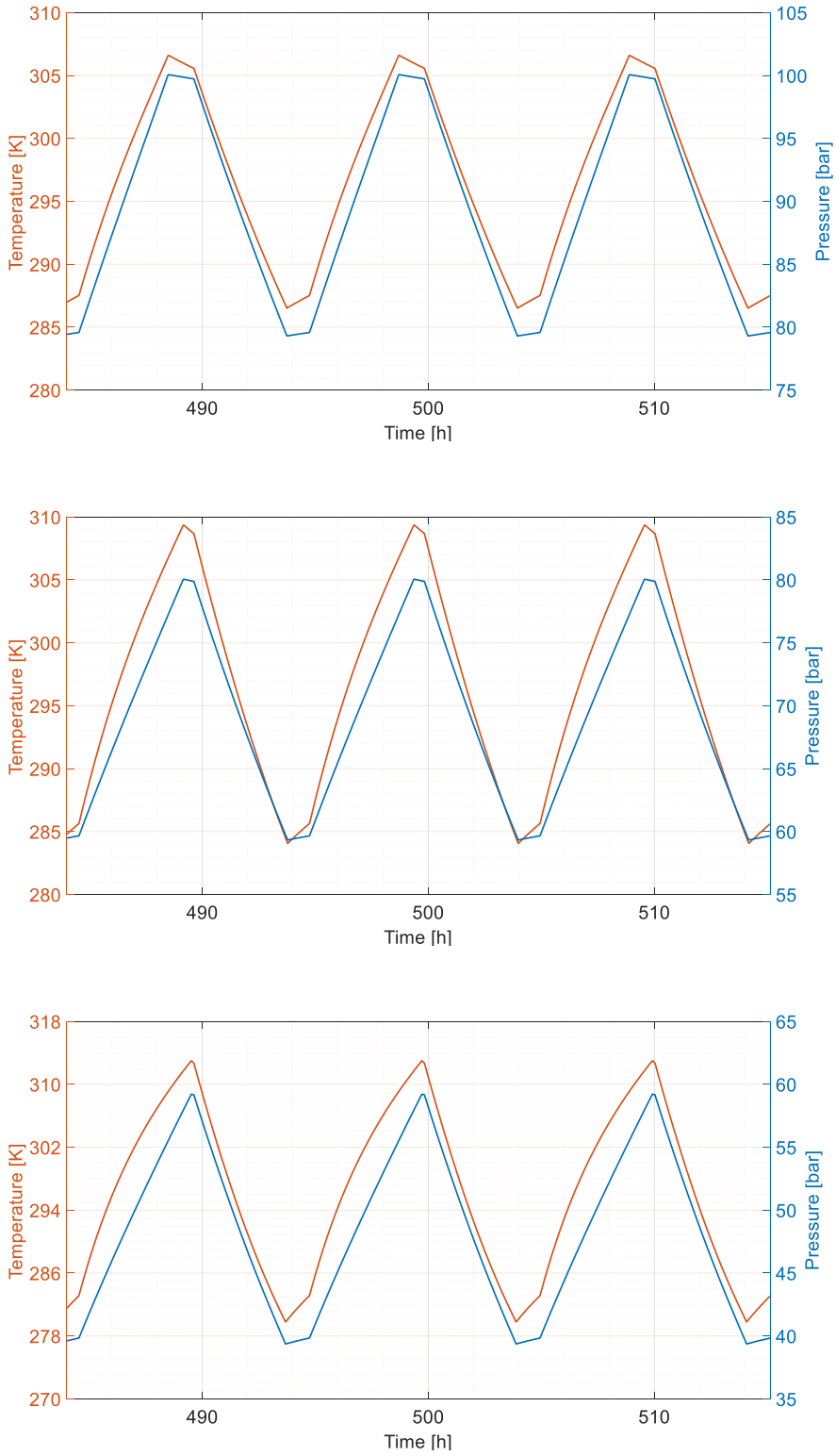


**Figure 36: Temperature and pressure in the cavern during the last 3 cycles. From top to bottom: maximum cavern pressure set at 100, 80 and 60 bar.**

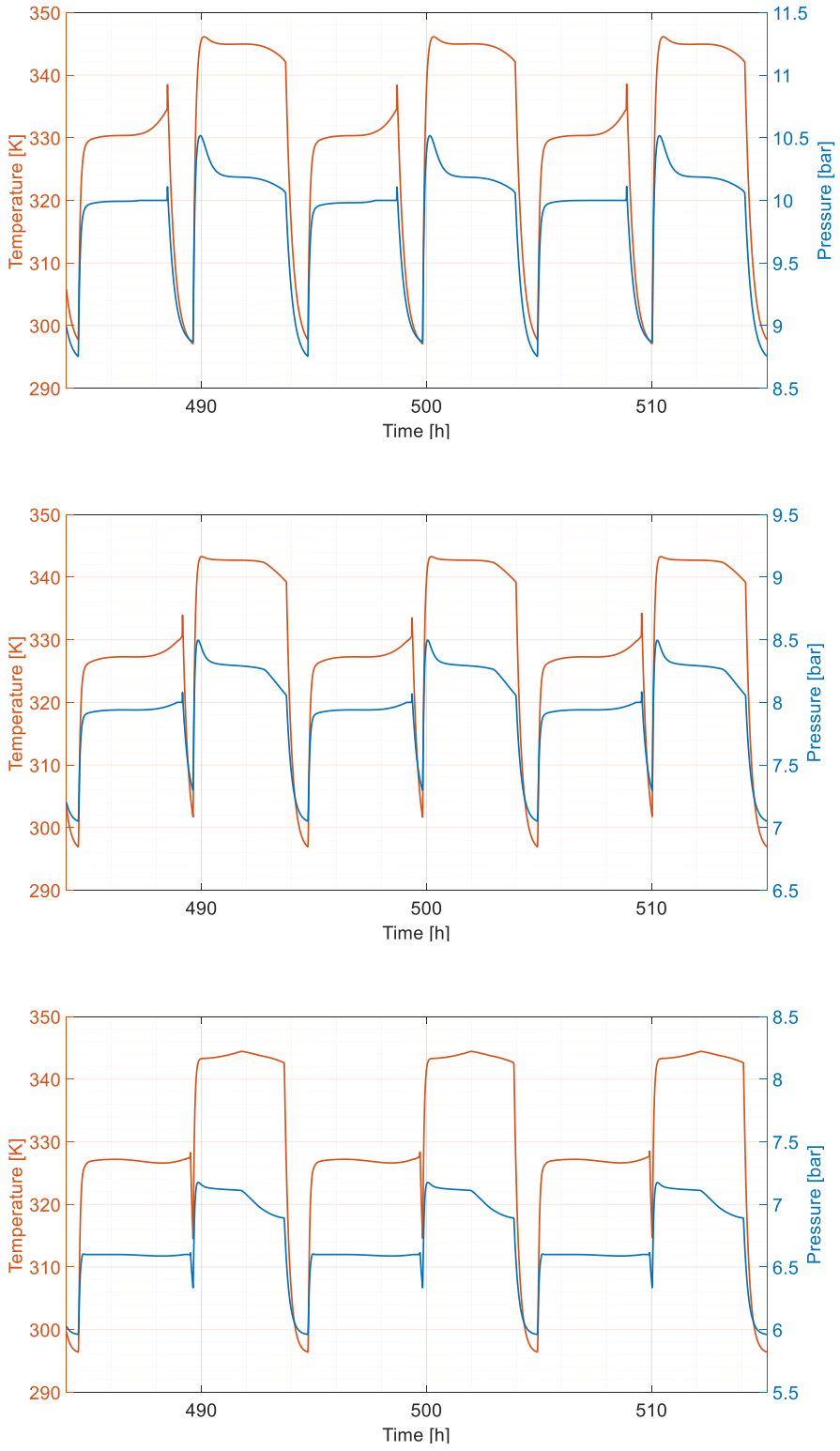


**Figure 37: Temperature and pressure in the TES chamber during the last 3 cycles. From top to bottom: maximum cavern pressure set at 100, 80 and 60 bar.**

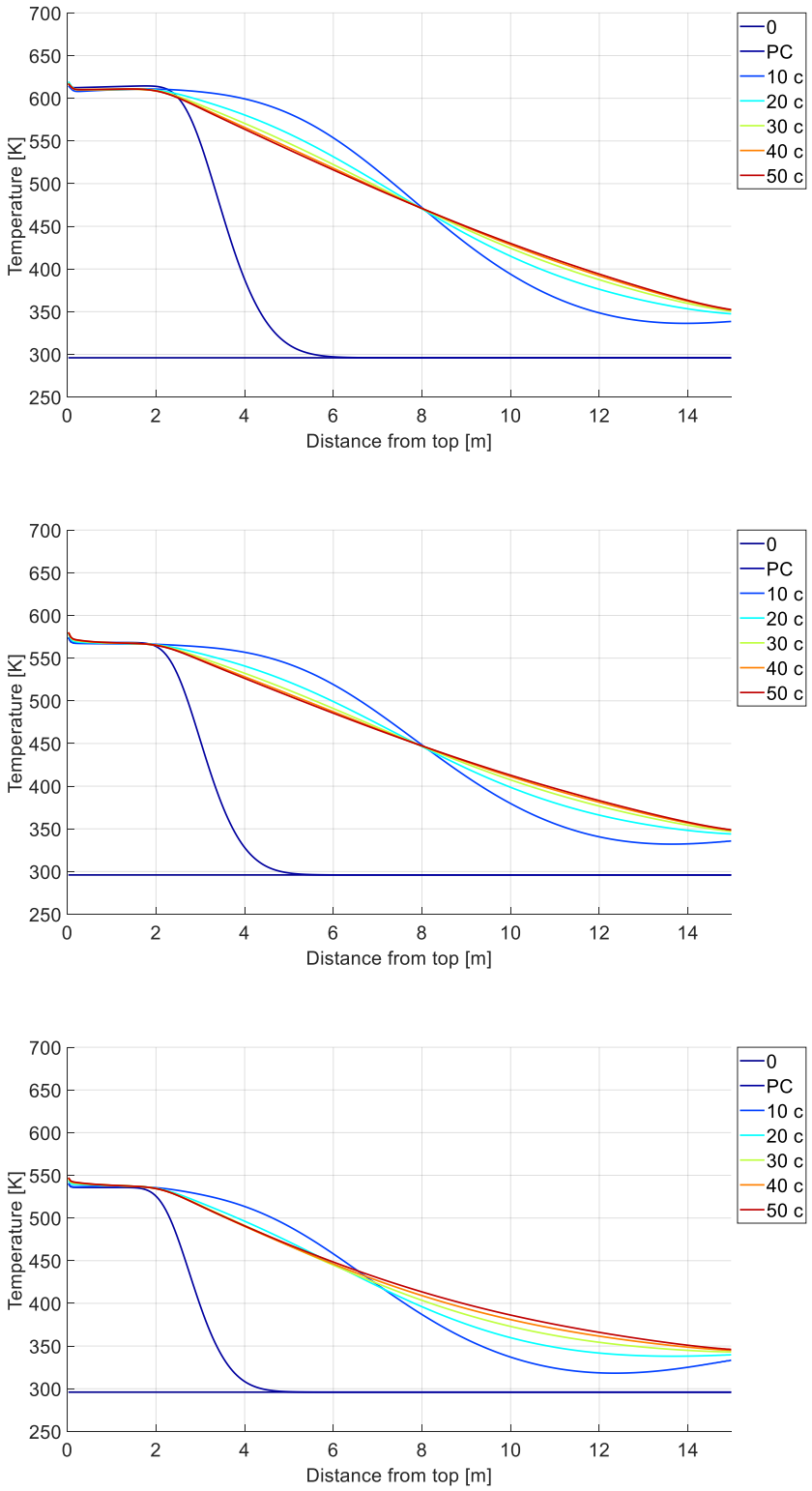


**Figure 38: Thermoclines at the end of the charge phases, LP TES.**
**From top to bottom: maximum cavern pressure set at 100, 80 and 60 bar.**

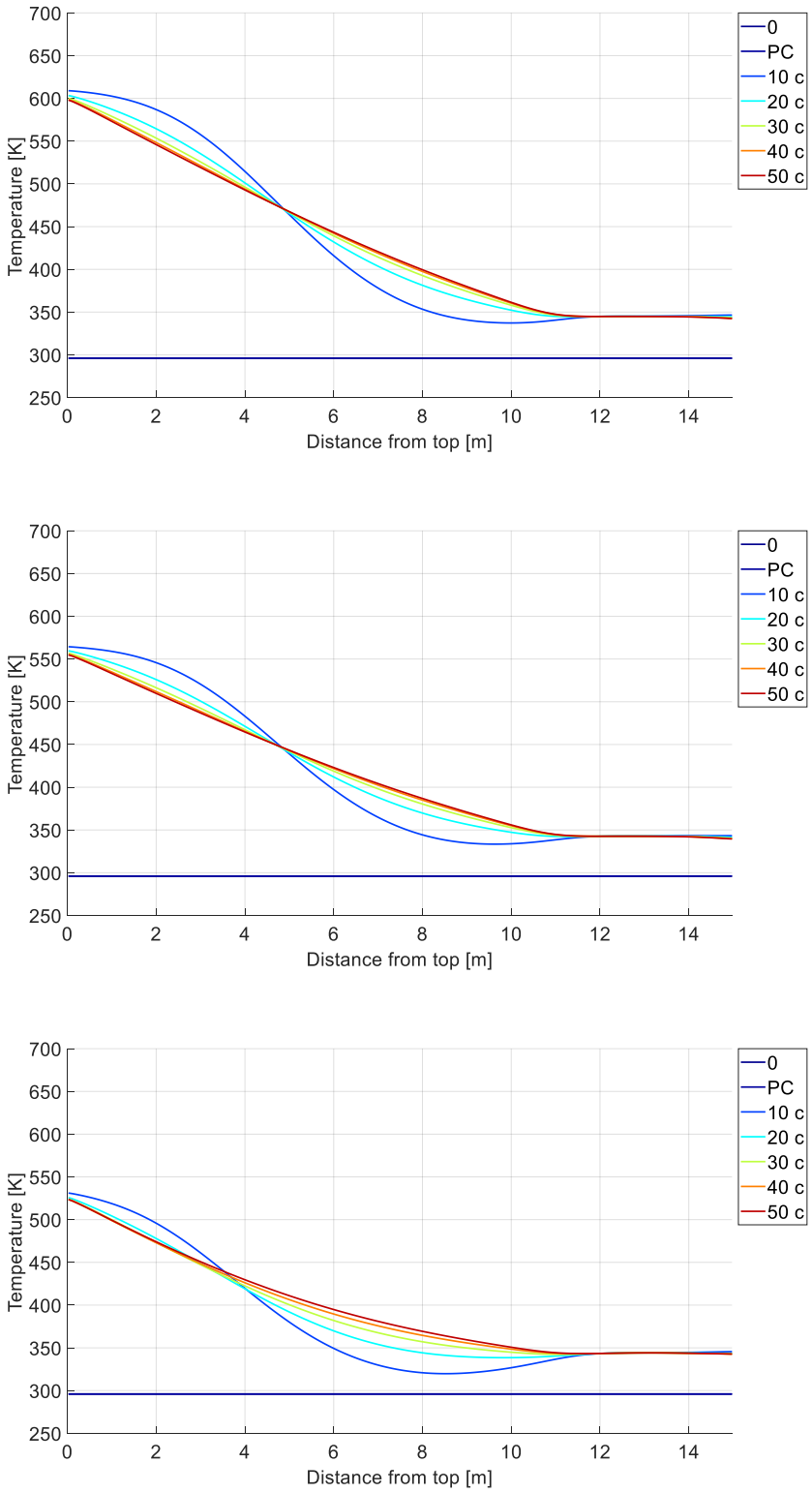


**Figure 39: Thermoclines at the end of the discharge phases, LP TES. From top to bottom: maximum cavern pressure set at 100, 80 and 60 bar.**

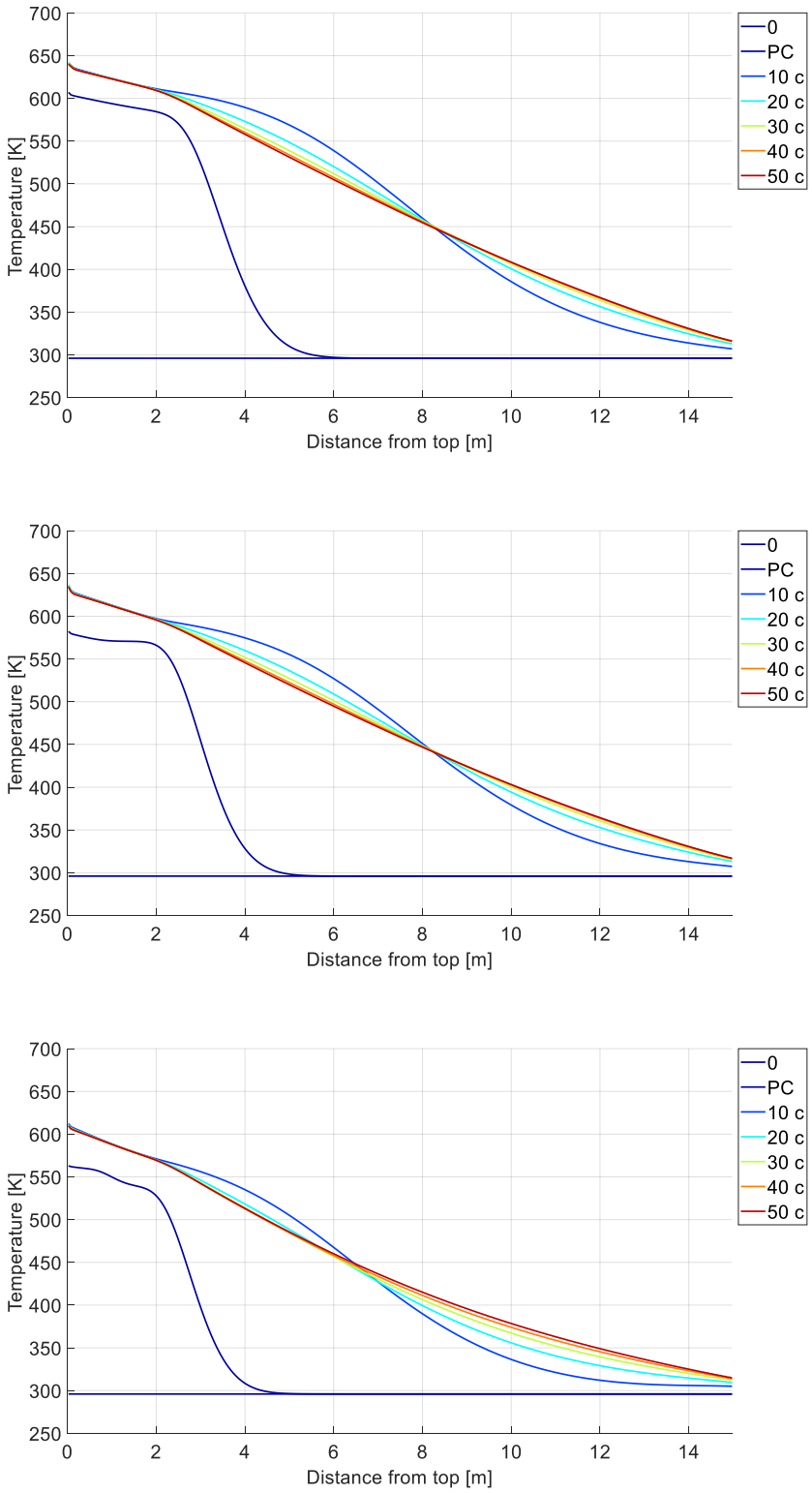


**Figure 40: Thermoclines at the end of the charge phases, HP TES.**
**From top to bottom: maximum cavern pressure set at 100, 80 and 60 bar.**

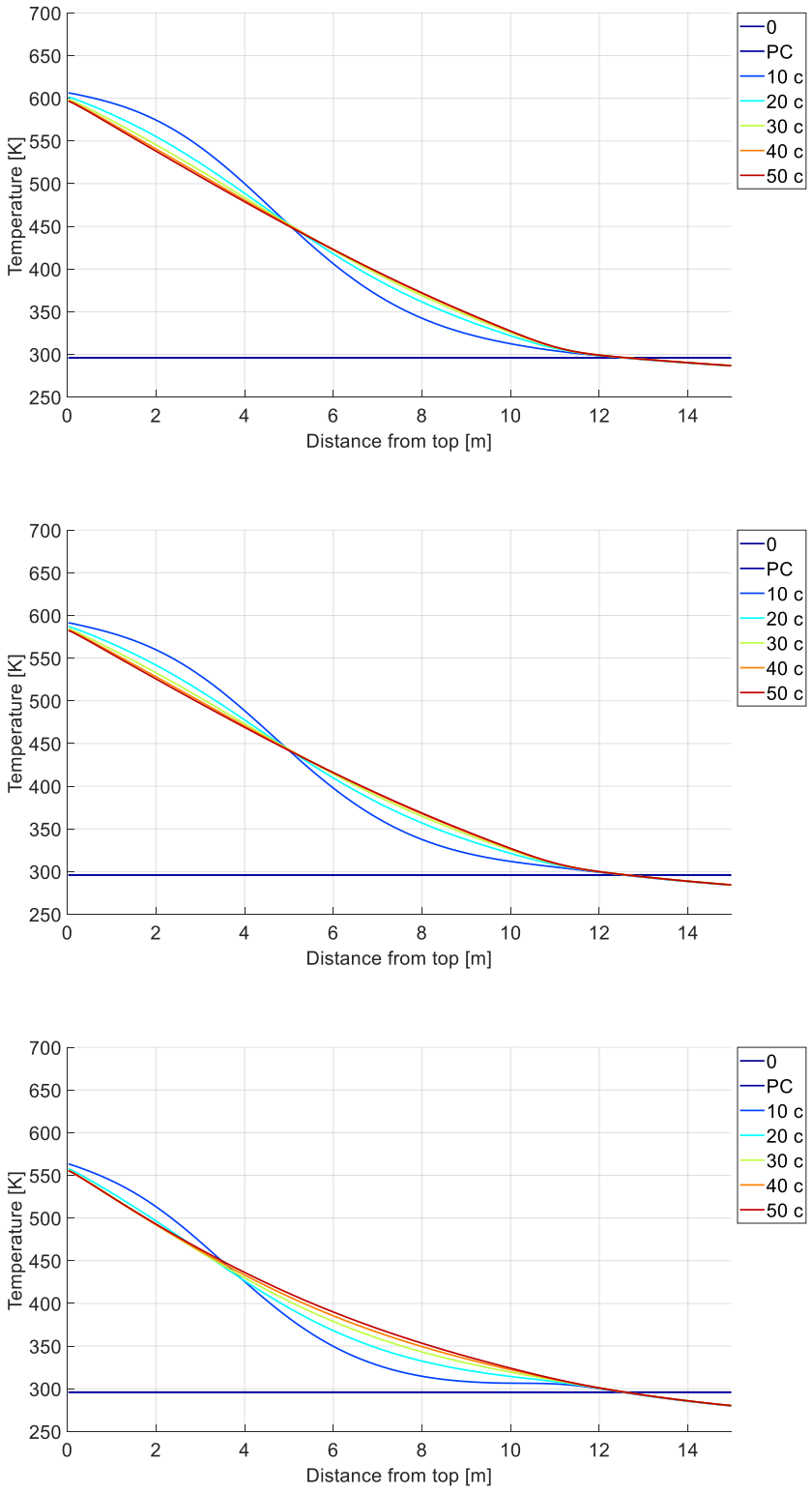


**Figure 41: Thermoclines at the end of the discharge phases, HP TES. From top to bottom: maximum cavern pressure set at 100, 80 and 60 bar.**

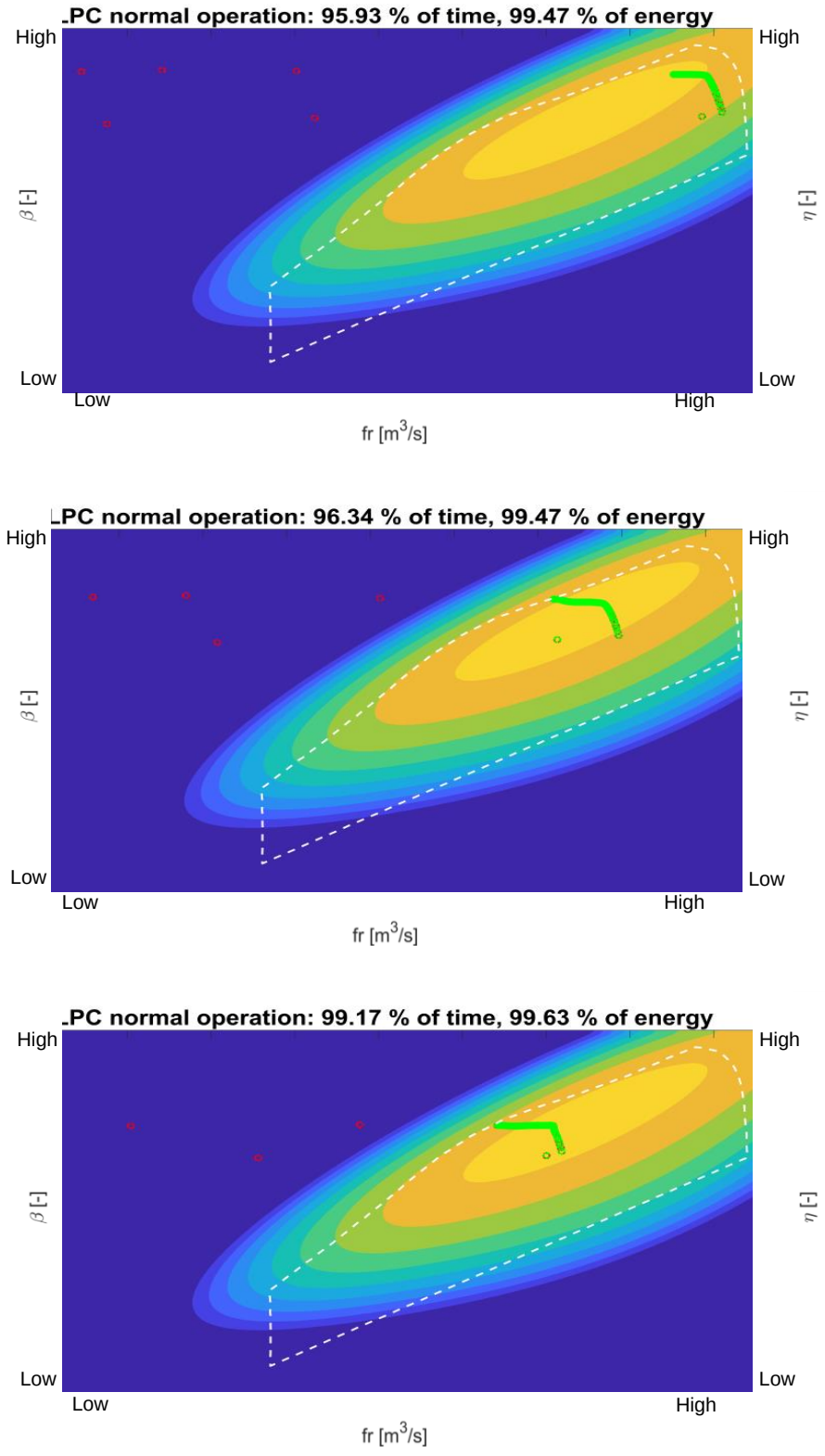


**Figure 42: Operating points of the LPC during the last cycle superimposed on efficiency contour. Red circles are outside the normal operating region, green ones are inside.**
**From top to bottom: maximum cavern pressure set at 100, 80 and 60 bar.**

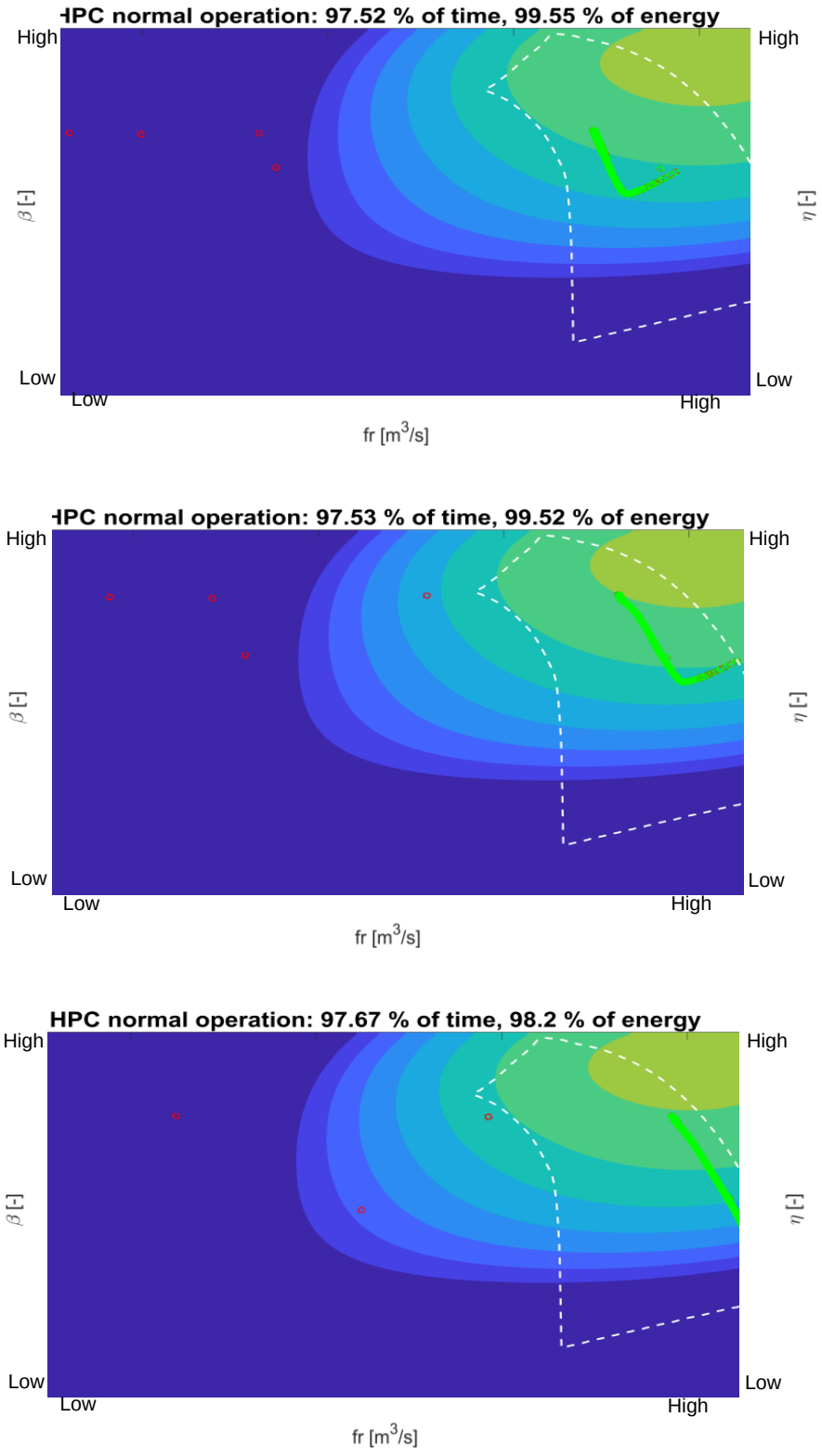


**Figure 43: Operating points of the HPC during the last cycle superimposed on efficiency contour. Red circles are outside the normal operating region, green ones are inside.**
**From top to bottom: maximum cavern pressure set at 100, 80 and 60 bar.**

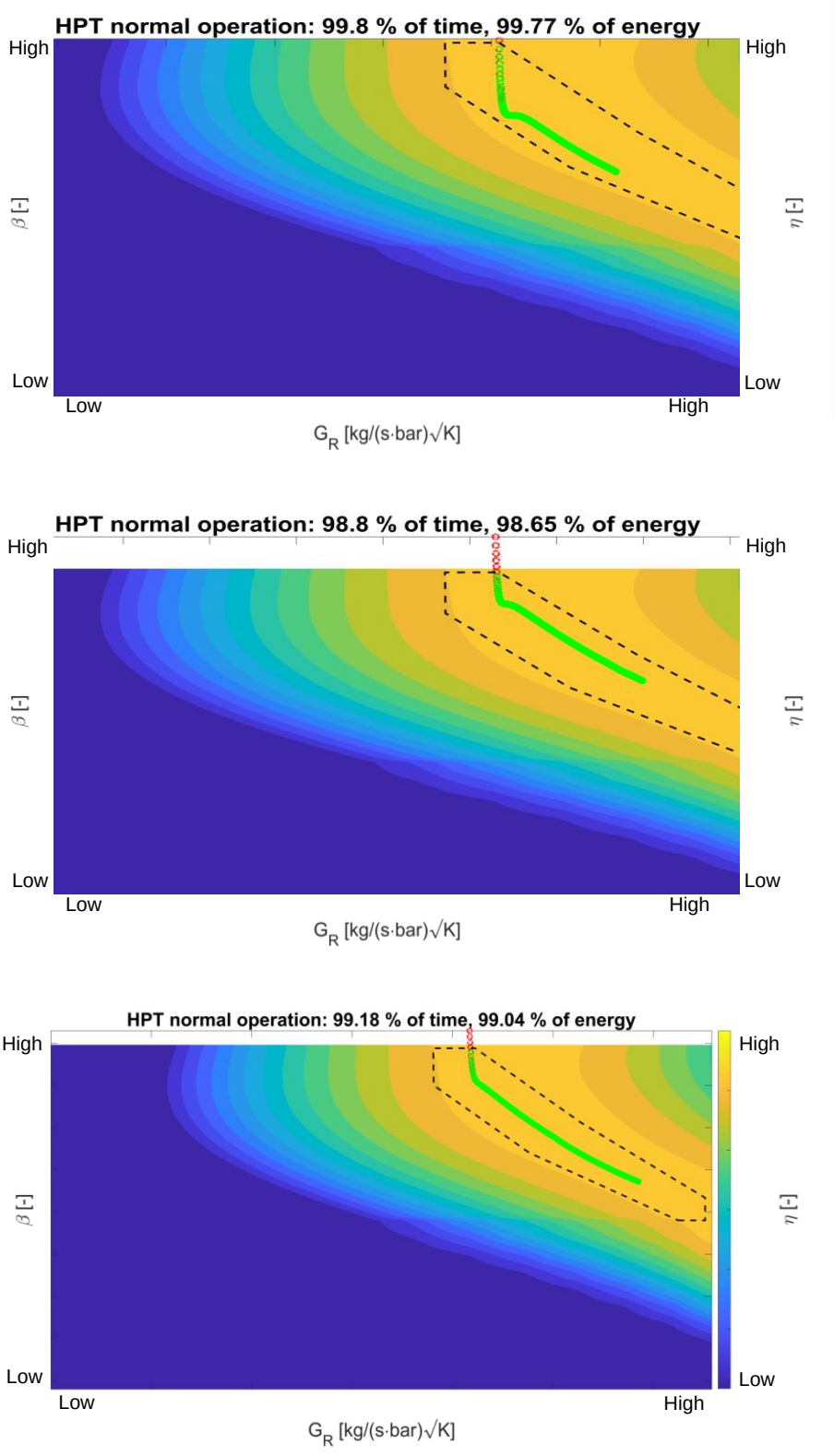


**Figure 44: Operating points of the HPT during the last cycle superimposed on efficiency contour. Red circles are outside the normal operating region, green ones are inside.**
**From top to bottom: maximum cavern pressure set at 100, 80 and 60 bar.**

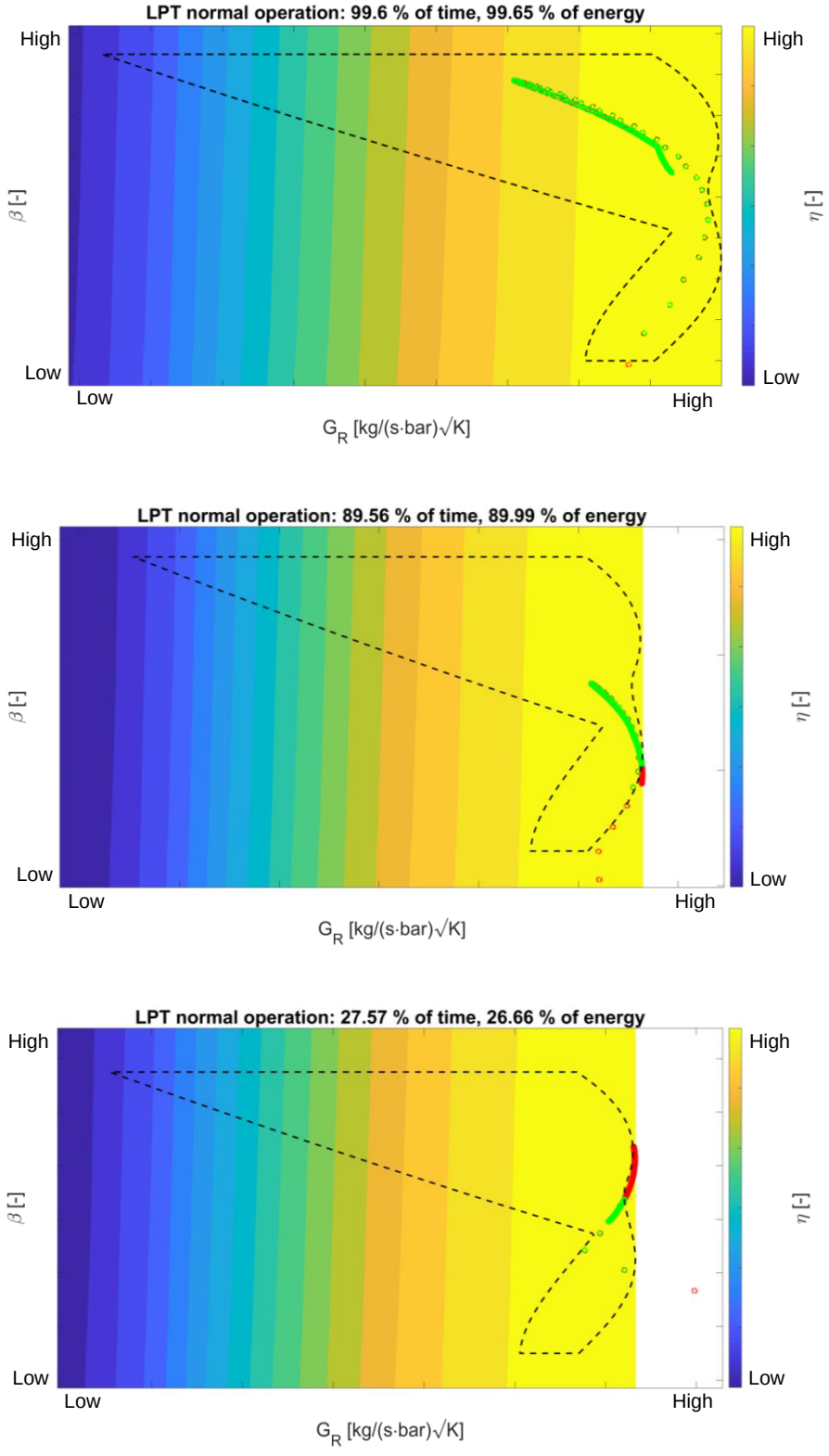


**Figure 45: Operating points of the LPT during the last cycle superimposed on efficiency contour. Red circles are outside the normal operating region, green ones are inside.**
**From top to bottom: maximum cavern pressure set at 100, 80 and 60 bar.**

## 6.3 Sensitivity to air properties: adapted polytropic efficiency

Efficiency maps provided by MAN ES were directly implemented into the AA-CAES model with generally good accordance on the outlet temperatures of compressors and turbines. Unfortunately, in some cases the deviations might be significant (see Figure 46) and therefore their influence over the AA-CAES performance was investigated. This discrepancy can be due to a difference between the air properties used in the model and those used to perform the efficiency evaluation at MAN. Therefore, the polytropic efficiencies of compressors and turbines were recalculated using the same dry-air temperature dependent properties used in the numerical simulation (see Equations (13) and (14)). The model was then applied again with the recalculated values to evaluate the effects on the AA-CAES plant performance.

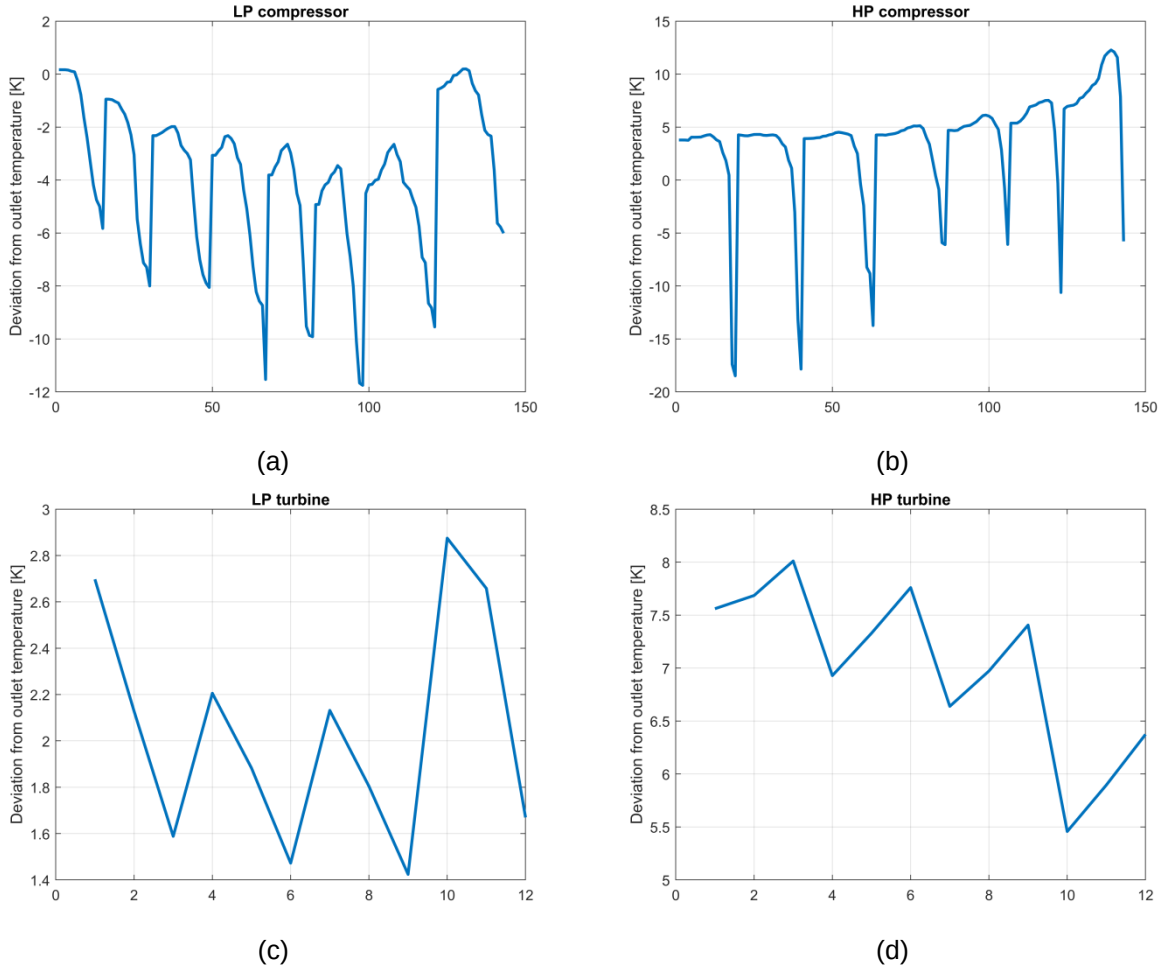


**Figure 46: Temperature difference between the data provided by MAN ES and the outlet temperatures determined by the numerical model. Data on the abscissa are the available data ID.**

$$\eta_{pol,c} = \frac{\gamma - 1}{\gamma} \frac{ln(p_2/p_1)}{ln(T_2/T_1)} \tag{13}$$

$$\eta_{pol,t} = \frac{\gamma}{\gamma - 1} \frac{ln(T_2/T_1)}{ln(p_2/p_1)} \tag{14}$$

An interesting comparison of the plant efficiencies can be done looking at Table 8: they are almost constant moving from 60 bar towards 100 bar (60A – 100A) but, if compared to the originals cases, they decreased, on average, by 1.6%. The main cause can be found in the reduced power extracted during the discharging phases, as highlighted in Table 9, where the results gathered from the original efficiencies (60 - 100) are confronted with those from the adapted ones (60A - 100A). Moreover, Table 10 reports an analogous comparison based on the mass flow rates which highlights that in cases 60A - 100A compressors processed less air. Hence, having kept the same pressure ranges, the compressor time operation increased. Having fixed also the total power, the increased energy required during charges further impacts negatively on the AA-CAES plant efficiency.

**Table 8: Plant overall efficiency comparison between the original (left) and adapted $\eta$ (right). The rightmost column reports the efficiency difference.**

| | $\eta$ [−] | | | |
|---|---|---|---|---|
| **60** | 74.6 | **60A** | 73.3 | -1.3 |
| **80** | 75.5 | **80A** | 74.0 | -1.5 |
| **100** | 75.1 | **100A** | 73.1 | -2.0 |

**Table 9: Turbine powers and percentage variation during the last cycle. Comparison between the original polytropic efficiencies (60, 80, 100) and the adapted ones (60A, 80A, 100A).**

| | LP Turbine [MW] | | HP Turbine [MW] | | Turbine Train [MW] | |
|---|---|---|---|---|---|---|
| | start | end | start | end | start | end |
| **60** | 43.77 | 40.52 | 52.18 | 38.48 | 95.95 | 79.00 |
| **80** | 49.74 | 45.84 | 57.10 | 45.19 | 106.84 | 91.03 |
| **100** | 56.20 | 54.27 | 58.20 | 48.12 | 114.40 | 102.39 |
| **60A** | 43.34 | 39.74 | 51.13 | 37.94 | 94.47 | 77.68 |
| **80A** | 49.24 | 45.19 | 56.02 | 44.60 | 105.26 | 89.79 |
| **100A** | 55.48 | 53.67 | 57.61 | 47.84 | 113.09 | 101.51 |
| | -0.98% | -1.92% | -2.01% | -1.40% | -1.54% | -1.67% |
| | -1.01% | -1.42% | -1.89% | -1.31% | -1.48% | -1.36% |
| | -1.28% | -1.11% | -1.01% | -0.58% | -1.15% | -0.86% |

**Table 10: Compressor mass flow rate and percentage variation during the last cycle. Comparison between the original polytropic efficiencies (60, 80, 100) and the adapted ones (60A, 80A, 100A).**

| | LP compressor [kg/s] | | HP compressor [kg/s] | | HP turbine [kg/s] | | LP turbine [kg/s] | |
|---|---|---|---|---|---|---|---|---|
| | start | end | start | end | start | end | start | end |
| **60-60A** | 0.53% | -0.26% | -0.00% | -0.26% | -0.00% | -0.20% | 0.30% | -0.31% |
| **80-80A** | -0.11% | -0.52% | -0.54% | -0.75% | -0.00% | -0.05% | 0.40% | -0.05% |
| **100-100A** | -0.65% | -0.93% | -1.13% | -1.03% | -0.00% | -0.00% | -0.05% | -0.05% |

## 6.4 Plant performance sensitivity to cycle duration

Analyzing the result gathered including real turbomachinery behavior in the simulations, it seemed that the energy spent during turbomachinery start-ups and stops was always negligible compared to the amount consumed and dispatched during normal plant operation. A sensitivity analysis was done to figure out if the cycle duration (i.e., the length of charges and discharges) and the turbomachinery power would affect the AA-CAES plant efficiency, including auxiliary turbomachinery consumptions.

Due to the large number of variables involved in the model and the necessity to tune properly the turbomachinery maps in order to have comparable results, a simplified evaluation was conceived to better identify the effects of each parameter change. The power input for the set of AA-CAES plant simulations was 140 MW, 100 MW and 90 MW. Assuming an assigned AA-CAES plant efficiency and an equal time duration for both the charge and discharge phases, the output power was defined. From these data, and using the start-up and stop powers, the corrected efficiency including them can be determined.

Figure 47 depicts two plots that summarize the effects of AA-CAES plant efficiency, cycle duration and charge power on the difference between the AA-CAES plant efficiency itself (turbine energy over compressor energy) and the AA-CAES plant efficiency including the energy consumptions for turbomachinery transients and stops.

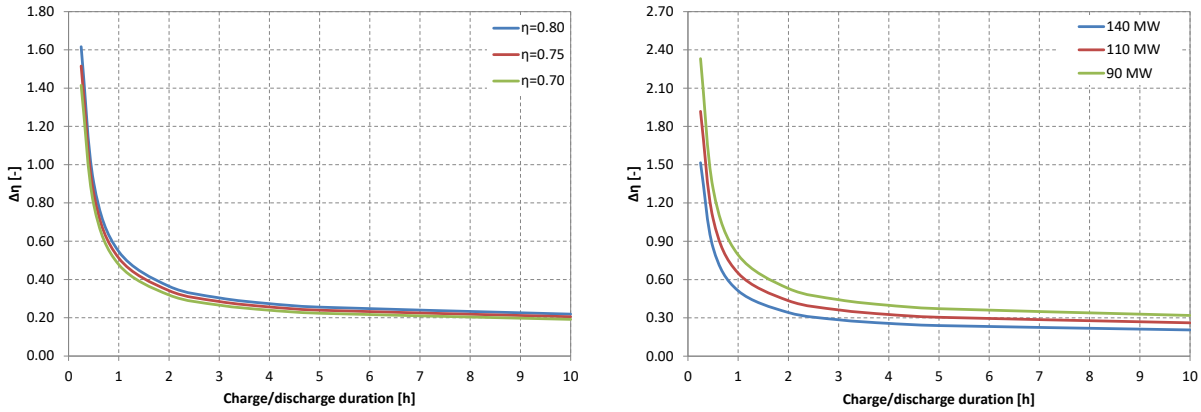


**Figure 47: Effect of start and stops: variation of plant efficiency vs cycles duration. On the l.h.s the curve parameter is the AA-CAES efficiency; on the r.h.s. the influence of the charge power is considered.**

The left-hand side of Figure 47 shows the efficiency difference as function of the cycle duration (proportional to charge/discharge length) and parametrized by the assumed AA-CAES plant efficiency for a full-scale plant (140 MW during charges). For charges and discharges lasting 5 hours, as those exploited in the simulations presented in Section 6.1, the impact of the start-ups and stop powers is limited. For longer cycles the influence is further lowered while shortening the duration has a significant effect on increasing the efficiency difference (a positive delta means reduction of efficiency). This was caused by the reduced amount of energy elaborated by the plant with respect to the one consumed during transients and stops. The same consideration is valid for the plot on the right-hand side of Figure 47, which depicts the same efficiency difference parametrized by the AA-CAES plant size: lowering the power of the plant notably increases the delta (a positive delta means reduction of efficiency).
Looking at the results summarized in Figure 47, a threshold can be identified in charge and discharge lengths of 2 hours: for longer cycles the impact of turbomachinery auxiliary energy slowly decreases but for shorter cycles it sensibly affects the AA-CAES plant performance. This detrimental consequence is further amplified in downscaled power sizes as shown on the r.h.s. of Figure 47.
Considering the sample points chosen to check the validity of these results, the discrepancy between the efficiency difference estimated with this simplified approach and a detailed simulation was below 15%.
As a final consideration, it must be noticed that also the duration of the turbomachinery stops themselves directly impacts on the plant efficiency, contributing to increase the amount of energy to be spend to keep the plant in stand-by but responsive to the electric grid requests.

# 7 Conclusions and perspectives

## 7.1. Modeling

The numerical model suitable for AA-CAES plants simulations developed at SUPSI was extended so to include real turbomachinery efficiency maps and auxiliary energy consumption (due to transients and stand-by) in order to have an instrument capable of evaluating the grid-to-grid performance of such storage plants. In order to fulfil this goal, the layout of the plant to be studied was designed based on the contribution of all project partners namely, SUPSI, MAN Energy Solutions Schweiz AG, ALACAES and ETHZ. The most feasible solution identified was to have a compression train with the overall compression ratio evenly divided between two compressors. Doing the same also for the expansion train the plant required to include two TES, one for each stage. The LP-TES is contained in a separate pressurized chamber, whereas the HP-TES is located in the cavern where the high pressure air is stored.

Therefore, the analysis focused on three different plant operation conditions for the fixed layout, each of which was characterized by a cavern pressure range: 80 to 100 bar, 60 to 80 bar and 40 to 60 bar.
MAN ES turbomachinery components were designed upon the AA-CAES plant operating conditions in the highest pressure layout; for the lower pressure ones, the original turbomachinery components were downscaled to fit the new operating conditions.
The simulations served to define the expected efficiency of these plant configurations and to analyze the model sensitivity to thermophysical properties of the air, cycle duration and power ratings.

From the studies performed in this project, the main findings are:

1. the AA-CAES plant efficiency is generally not heavily influenced by the pressure level adopted, since in all the three layouts analysed the overall efficiency was close to 75%.
2. The start-up energies of the compressor and turbine trains were taken into account in the post-processing of the dynamic results. Their influence on the AA-CAES plant efficiency was secondary but, as revealed by a sensitivity analysis, they can become more significant the shorter the cycles and the lower the turbomachinery power. Therefore, auxiliary turbomachinery consumptions should be considered to properly schedule the AA-CAES plant operation: this statement is of paramount importance looking at the daily schedule of power plants, whose everyday timetables are defined with 15 minutes time steps, based on market electric energy demand.
3. The AA-CAES plant efficiency is considerably affected by the turbomachinery polytropic efficiencies. The same layouts analysed with the adapted polytropic efficiencies (calculated to better fit the declared outlet temperatures of MAN ES turbomachinery) showed a decrease of 1.6% (on average). Due to the significant sensitivity to air properties, it would be interesting to further develop the model to include air humidity and real gas behaviour for air. The former will also give a clue to quantify collateral effects of the process such as the amount of water condensed within the TESs during air cooling and the effect of different mass flow rates passing throughout different machines.

## 7.2. Turbomachinery

Inclusion of detailed performance maps of turbomachinery into the dynamic simulation model made possible to upgrade and enhance the existing plant design tool. The MAN ES turbomachines considered are items effectively available and dimensioned appositely for the AA-CAES plant needs. This approach gave a unique feature to the plant simulation model that is now applicable to evaluate grid-to-grid AA-CAES plant performance. Furthermore, with these data, a realistic estimation of plant CAPEX was possible.

### 7.2.1. Transient turbomachinery behavior

Effects of transient turbomachinery behavior during start-up and shut-down phase were analyzed. A detailed study of MAN ES machines shows quantitative data about time, power, and energy consumption during these phases. These data were implemented in the AA-CAES plant model and used to evaluate plant efficiency accounting for turbomachinery consumption during these transients and during idle phases. In particular, the study concluded that the warm operating mode (namely, slow roll mode) of the turbomachines between two cycles seems to be the most attractive option. In fact, the energy requirements for keeping the turbines and compressors in the slow roll mode are relatively low and are expected to predominate the long start-up times from cold starts.
Transients influence on the AA-CAES plant efficiency was found secondary but, as revealed by the sensitivity analysis, it can become more significant the shorter the cycles and the lower the turbomachinery power.

### 7.2.2. Combined compressor and expander solutions

From the analysis performed by MAN ES and from their investigation of the existing technologies, it appears that a compression-expansion combined machine, if available, cannot offer the performance for large AA-CAES plants.

For a combined compressor/expander machine, based on turbomachinery, an analysis of several technical solutions was performed.

The application of radial compressor stages also for expansion revealed some issues. In particular:

- A different sense of rotation for compression and expansion.
- The pressure ratio per each stage is probably limited by the compression purpose.
- The average efficiency for compression and expansion is seen as a major challenge.
- At the moment, no industrial application is known.
- The state of the art of these machines requires further basic research (low TRL).

When considering axial machines, at the state of the art, no concept is known to use (modified) axial compressors as turbines with high overall efficiency.

Still remaining on systems based on turbomachinery, two further technical solutions were considered, provided different blading for compression and expansion are used.

- Multi stage geared compressor and expanders. They imply some challenges, in particular:
  - determine what the compression stage is doing while the system discharging. The same problem occurs to the expander during the charge phase.

- Another point to consider is that radial turbomachinery is less efficient and more expensive than axial turbomachinery when high Power (> 50 MW) is concerned. Furthermore, this technology is not available for all options.

- Compressor motor/generator and turbine in one train. This is not a real single machine, but a combination of several turbomachinery. In this case the challenges are:
  - A complicated clutch system is required, e.g., a synchronized self shifting clutch.
  - The very long trains limit the operational flexibility.
  - The last point to consider is the system complexity and its consequent reliability.

As possible alternative to turbomachinery, a system based on piston compressor/expander with active valve control was considered. In this case, the challenge to face is mainly the fact that there are not such systems suitable for the high power and high mass flow rates found in the AA-CAES plants considered here. Cost effective scalability to very large scales of energy storage plants seems very questionable at this stage. They can work for laboratory size and small plants.

## 7.3. AA-CAES plant siting

To locate the high pressure air storage volume, the exploitation of unused military cavern was excluded because:

- the caverns do not have sufficient overburden to contain the maximum cavern pressures of about 100 bar.
- The caverns typically have multiple entrances and exits, all of which represent potential paths for air to leak from the cavern.
- The caverns are typically highly branched, leading to large surface-to-volume ratios, which would increase heat losses from the compressed air to the surrounding rock.
- The cross-section of most of the caverns is horseshoe-shaped, which may induce stress concentrations and consequent fracturing and air leaks.
- Few caverns were located in regions with high-quality rock (the Aare massif), and they would therefore likely have required costly measures to render them airtight.

The plant-siting study has then moved the attention to excavating entirely new caverns. The financial consequences of this decision on the profitability of AA-CAES plants in Switzerland will be investigated in the parallel ongoing SCCER HaE AA-CAES project.

## 7.4. Grid

AA-CAES detailed dynamic model cannot be directly embedded into models that simulate interconnected electricity systems that, for a realistic analysis of the Swiss grid, must include also Germany, France, Italy, and Austria. This grid simulation software can instead exploit results of the detailed AA-CAES model, therefore a soft coupling is foreseen.

## 7.5. AA-CAES plant costs

The base case of the cost model was set up for a plant with 100 MW power (100 MW discharging, 135 MW charging) and 500 MWh capacity with the cavern excavated in Swiss Alpine rocks. The capital expenditure per kWh of installed capacity for this base case was evaluated as 200-300 €/kWh. The

civil works and the turbomachinery have by far the biggest share of the plant costs: 52% and 32% respectively. Thermal energy storages play just a 6% of it.
The presence of lower quality rocks would increase the CAPEX to 200-300 €/kWh due to more costs for structural support and possible smaller caverns.
In developing countries, a lowering of the CAPEX is envisaged due to the lower cost of civil and construction works.
A comparison with pumped hydro storage systems showed that AA-CAES has:

- lower CAPEX
- lower efficiency (75% vs 85%)
- significantly smaller environmental footprint
- similar cycle lifetime

Furthermore, looking at the ESOI, i.e., the Energy Stored on Invested, that represents the ratio of electrical energy stored over the lifetime of a storage device to the amount of primary embodied energy required to build the device, AA-CAES systems offer a value of 240 vs 210 of Pumped Hydro and 10 of Li-ion batteries. This is a quite significant results when looking at system sustainability.

## 7.6. Research perspectives

### 7.6.1. Modeling

Further modeling efforts should be focused on the following points:

- The study of the detailed plant under realistic power scenarios (coupling it with electric grid simulations), to verify the AA-CAES capabilities to respect the electric grid and efficiency requirements;
- Include air humidity and real gas behavior in both the plant numerical model and in the 1D TES code to quantify their effects on the plant performance and their collateral drawbacks. For example, evaluating the amount of water condensed within the LP TES during LP air cooling and the effect of different mass flow rates passing throughout different machines mounted on the same train.
- Include the piping between the components to evaluate plant performance considering also losses due to the pressure drop and heat dissipation.

### 7.6.2. Experimental activities

After the experiments performed by ALACAES and the studies produced by ETHZ and SUPSI, a series of experimental activities should be performed to explore:

- cavern tightness with the possibility of testing different rock lining.
- rock fatigue when realistic AA-CAES pressure cycling is considered.

At the actual stage of research an AA-CAES pilot plant realized in Switzerland can be the right opportunity to have all missing answers. Opportunities of realizing this goal with European Community collaboration should also be explored.

# Nomenclature

### Latin characters

| | | |
|---|---|---|
| $A$ | $m^2$ | area |
| $G_R$ | kg√K/(s·bar) | reduced mass flow rate |
| $h$ | J/kg | enthalpy |
| $h_c$ | $W/m^2K$ | convective heat transfer coefficient |
| $M$ | kg | mass |
| $\dot{m}$ | kg/s | mass flow rate |
| $\dot{P}_C$ | W | compressor power |
| $\dot{P}_T$ | W | turbine power |
| $T$ | K | temperature |
| $T_{cr}$ | K | critical temperature |
| $T_R$ | - | reduced temperature |
| $t$ | s | time |
| $p$ | Pa | pressure |
| $p_{cr}$ | Pa | critical pressure |
| $p_R$ | - | reduced pressure |
| $\dot{Q}_{TES}$ | W | TES thermal losses |
| $U$ | J | internal energy |

### Greek characters

| | | |
|---|---|---|
| $\beta$ | - | compression ratio ($p_{max}/p_{min}$) |
| $\gamma$ | - | specific heat ratio |
| $\eta_{is}$ | - | isentropic efficiency |
| $\eta$ | - | polytropic efficiency |
| $\eta_m$ | - | mechanical efficiency of motor/generator |

### Abbreviations

| | |
|---|---|
| AA-CAES | Advanced Adiabatic Compressed Air Energy Storage |
| CAES | Compressed Air Energy Storage |
| HP | High pressure |
| HPC | High pressure compressor |
| HPT | High pressure turbine |
| LP | Low pressure |
| LPC | Low pressure compressor |
| LPT | Low pressure turbine |
| MAN ES | MAN Energy Solutions Schweiz AG |
| PHS | Pumped Hydro Systems |
| TES | Thermal Energy Storage |

# References


[1] Y. A. Çengel and M. A. Boles, Thermodynamics, an Engineering Approach - 8th ed, McGraw Hill, 2015.

[2] P. Roos, J. Roncolato, M. Barbato, J. Garrison, A. Fuchs, T. Demiray, T. Motmans, W. Schenler, A. Haselbacher, A. Steinfeld, G. Zanganeh, P. Jenny, M. Scholtysik, E. Jacquemoud, F. Amberg, F. Pacher, J. Mühlethaler and M. Arnal, "Investigation of AA-CAES Plant Configurations and Grid Integration," SCCER HaE Annual Report 2017, pp. 65-67, 2017.

[3] C.J. Barnhart and S.M. Benson, “On the importance of reducing the energetic and material demands of electrical energy storage”, Energy & Environmental Science, 6, 1083, 2013.

[4] J. Garrison, A. Fuchs and T. Demiray, "Evaluating the grid and economic impact of AA-CAES in Switzerland," Future Electricity Networks, Energy Science Center, ETH Zurich, Zurich, 2017.

[5] Schlecht and H. Weigt, "Swissmod - A model of the Swiss electricity market," Forschungsstelle für eine nachhaltige Energie- und Wasserversorung, University of Basel, 2014.

[6] L. Geissbühler, A. Mathur, A. Mularczyk and A. Haselbacher, "An assessment of thermocline-control methods for packed-bed thermal-energy storage in CSP plants, Part 1: Method descriptions," Solar Energy, vol. 178, pp. 341-350, 2019.

[7] L. Geissbühler, A. Mathur, A. Mularczyk and A. Haselbacher, "An assessment of thermocline-control methods for packed-bed thermal-energy storage in CSP plants, Part 2: Assessment strategy and results," Solar Energy, vol. 178, pp. 351-364, 2019.

[8] P. Roos, J. Roncolato, F. Contestabile, S. Zavattoni, M. Barbato, J. Garrison, A. Fuchs, T. Demiray, C. Bauer, W. Schenler, P. Bugherr, A. Haselbacher, G. Zanganeh, P. Jenny, M. Scholtysik, E. Jacquemoud, A. Amberg, F. Pacher, J. Mühlethaler and M. Arnal, «Investigation of AA-CAES Plant Configurations and Grid Integration,» SCCER HaE Annual Report, pp. 60-63, 2018.

[9] J. Garrison, A. Fuchs and T. Demiray, "Joint economic evaluation coupling power grid and construction costs," Future Electricity Networks, Energy Science Center, ETH Zurich, Zurich, 2018.

[10] T. Motmans, "Environmental and Economic Assessment of Advanced Adiabatic Compressed Air Energy Storage," Master thesis, ETH Zurich, 2017.

[11] P. Roos and A. Haselbacher, “Sensible Thermal-Energy Storage Systems Optimized for AA-CAES Plant Operation”, SCCER HaE Annual Report, 2018.

[12] F. Crotogino, K. Mohmeyer, and R. Scharf, “Huntorf CAES: more than 20 years of successful operation”, In: Proc of SMRI spring meeting, Orlando, Florida, USA, 15–18; April 2001.

[13] https://idw-online.de/de/news671031 (visited May 8th, 2019).